ESD-TR-69-77

Technical Note

1969-15

Feasibility of Low Data Rate Mobile Troposcatter Communication Systems

D. P. White

30 April 1969

Prepared under Electronic Systems Division Contract AF 19(628)-5167 by

Lincoln Laboratory
MASSACHUSETTS INSTITUTE OF TECHNOLOGY
Lexington, Massachusetts

The work reported in this document was performed at Lincoln Laboratory, a center for research operated by Massachusetts Institute of Technology. The work was sponsored by the U.S. Navy under Air Force Contract AF 19(628)-5167.

MASSACHUSETTS INSTITUTE OF TECHNOLOGY

LINCOLN LABORATORY

FEASIBILITY OF LOW DATA RATE MOBILE TROPOSCATTER COMMUNICATION SYSTEMS

D. P. WHITE

Group 66

TECHNICAL NOTE 1969-15

30 APRIL 1969

LEXINGTON MASSACHUSETTS

ABSTRACT

For a communications system with a low data rate requirement (i.e., 1 - 1000 bits/sec) one can use troposcatter links over a range interval beyond the distances commonly used. The range is limited by the requirement that the tropopause layer is to be included in the common volume of the beams. This effectively limits the range in most cases to about 450 miles. It is proposed to use frequencies in the interval 3 to 5 GHz. This enables one to specify a completely mobile troposcatter system since the antenna paraboloids have diameters of the order of 10 feet and the power requirement is a modest 10 kW.

Accepted for the Air Force
Franklin C. Hudson
Chief, Lincoln Laboratory Office

TABLE OF CONTENTS

Feasibility of Low Data Rate Mobile Troposcatter Communication Systems

INTRODUCTION

During the last decade the utilization of tropospheric scatter communication systems for military purposes has increased substantially. In general these military systems can be characterized by moderately large receiver bandwidths (for multiple voice channels) and large stationary receiver and transmitter complexes. Links in the VHF band (50 -100MHz) provide troposcattered fields out typically to 600 miles beyond the radio-horizon. Links in the UHF and SHF bands (300MHz-5GHz) are typically used over ranges of the order of 100 to 300 km. For these large bandwidth systems the trade-off is primarily between larger antenna size and range.

However, if we are allowed to restrict our receiver bandwidths to a few KHz we can synthesize a class of troposcatter communication systems which have both small antenna size (antenna dish diameters of the order of a few meters) and moderately long range capability (links of the order of 720 km.). The penalty paid is that one is usually restricted to binary communication techniques with a moderately low information bit rate. We propose to use a FSK (frequency shift keying) modulation scheme. The benefits of such a troposcatter link are significant. If frequencies in the 3-6GHz region are used the transmitter and receiver complexes can be made mobile because of the small antennas and modest transmitter power requirements. Moreover at distances of the order of 640 km, the lower boundary of the common volume of the intersecting transmitter and receiver antenna beams is typically several kilometers above the earth's surface. The scattering region is then in the vicinity of 5 to 20 kilometers of altitude. Accordingly, the communications link will not be degraded by an adverse condition of the ionosphere. Finally, hardware needed for such a system is both relatively inexpensive and well within the present technological capability.

This report is divided into two parts. Part I is in part tutorial describing the nature of the atmosphere which is pertinent to our proposed troposcatter link. The effects of refraction are accounted for and diffraction is shown to be negligible. For computational purposes a hypothetical troposcatter link with a communications distance requirement of 400 miles (640 km) is selected.

Part II is concerned with the computation of the required transmitter power levels. In the various sections, sufficiently detailed analyses of the contributing terms are given permitting an eventual parameter study to decide on an 'optimum' system. The bulk of the report is concerned with this area.

I. Quantative Look at the Actual Troposcatter Geometry and the Common Volume Environment

In troposcatter systems analysis, the appropriate propagation equations (see Appendix A) are dependent only on the fine scale variations of the permittivity (or refractive index). However, these fine scale fluctuations are dependent on the gross meteorological conditions. The large scale refractive index behavior is described in Section A for its tutorial value. Then an approximation is used for dN/dh in order to compute the effects of normal refraction. By a suitable transformation the rays are "straightened" in Section B. Finally the beam geometry in relation to the actual path can be presented. A method for computing the scattering angle β is given.

If the reader is interested only in the system sizing considerations, he is advised to proceed directly to part II of this report.

A. Atmospheric Structure

In the design of transhorizon communication links, a relatively detailed knowledge of the atmospheric structure is essential. In particular the volume of atmosphere delineated by the intersection of the transmitter and receiver main lobe antenna beams is of paramount importance. In order to quantitatively describe the energy "scattered" out of this common volume it is necessary to estimate the structure of the refractive index variations both in time and space. This is necessary in order to catagorize whether the "scattering" mechanism is representative of specular reflection, diffuse reflection or the usual inhomogeneity scattering (or some combination of these processes).

It will be seen that for a 400 mile link the common volume will straddle the upper troposphere and the lower stratosphere (see Fig. 1). It is expected that refractive index fluctuations in the tropopause vicinity will give a significant received signal. This is in contrast to the usual shorter transhorizon links where most of the energy is scattered at altitudes below 5 km. Because the common volume of a 400 mile link is so high, very little of the vast

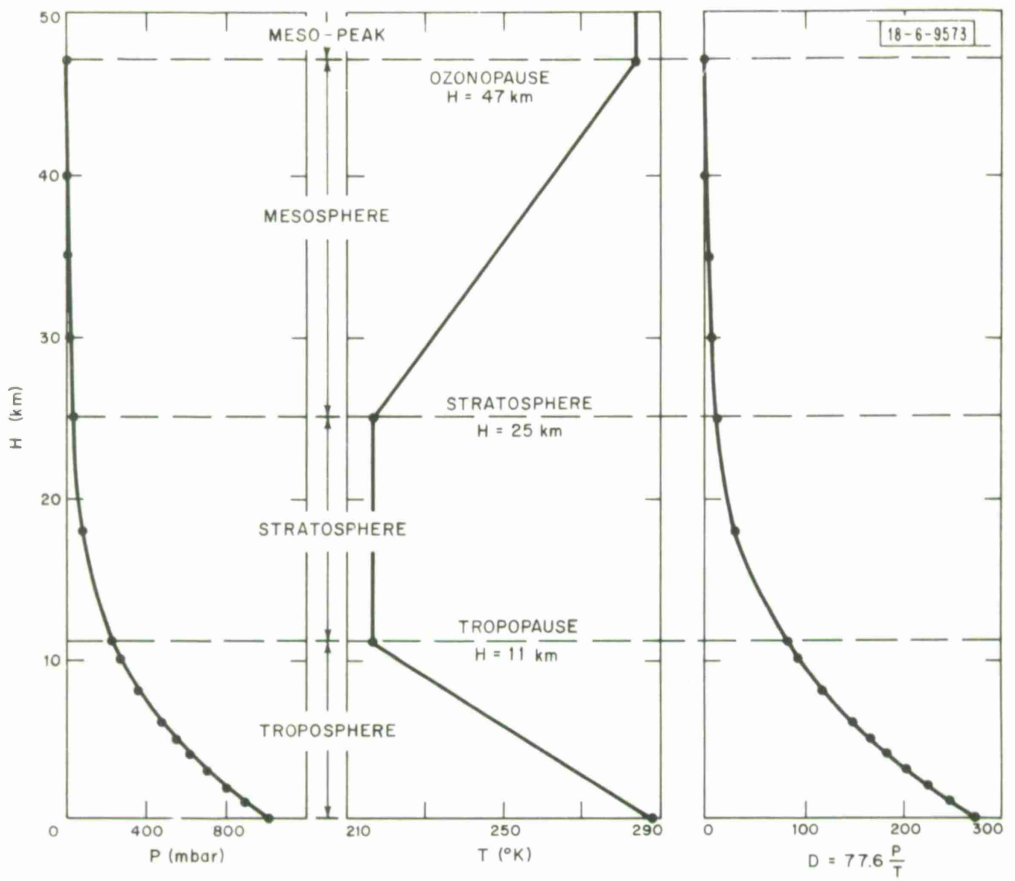

Fig. 1. The U.S. extension to the I.C.A.O. standard atmosphere.

amounts of experimental troposcatter data collected over the past decade is directly applicable. However, we can still size the system based on the limited experimental data available. If better estimates are desired it would be justified to perform some basic experimental research for links of this distance and operational frequency.

The refractive index structure will specify the type of radio wave propagation. For practical radio scatter applications the refractive index is usually described in terms of N units (rather than the refractive index η) where N is defined by [1],

$$N = (\eta - 1)10^{+6} \simeq 77.6 \frac{P}{T} - 5.6 \frac{e}{T} + 3.75 \times 10^5 \frac{e}{T^2} \qquad (1)$$

where e is the partial pressure of water vapor (mbars)

P is the total pressure

T is the temperature.

To a first approximation

$$N \cong 77.6 \frac{P}{T} + 3.75 \times 10^5 \frac{e}{T^2} \equiv D + W \qquad (2)$$

where D refers to the dry term and W to the wet term. Figure 2 [1] shows that only the dry term is important above an altitude of 5 km.* Of course, it is only the fluctuations in N (or D) that is of interest. Unfortunately, not many refractivity profiles in the upper troposphere and lower stratosphere are available by direct measurements (particularly the fine scale fluctuations). This being the case it is best to choose turbulence models which seem applicable at lower altitudes and check whether the limited long link experimental scatter data is consistent. It must be realized that the performance of a communications link is dependent on the gross(as compared to the fine scale turbulence) meteorological conditions which vary both diurnally and seasonally. For example there is evidence that strong scattering occurs in

*In short link troposcatter links it is the fluctuations in W that are dominant. For the longest links the D term is dominant and should be relatively insensitive to the actual path chosen.

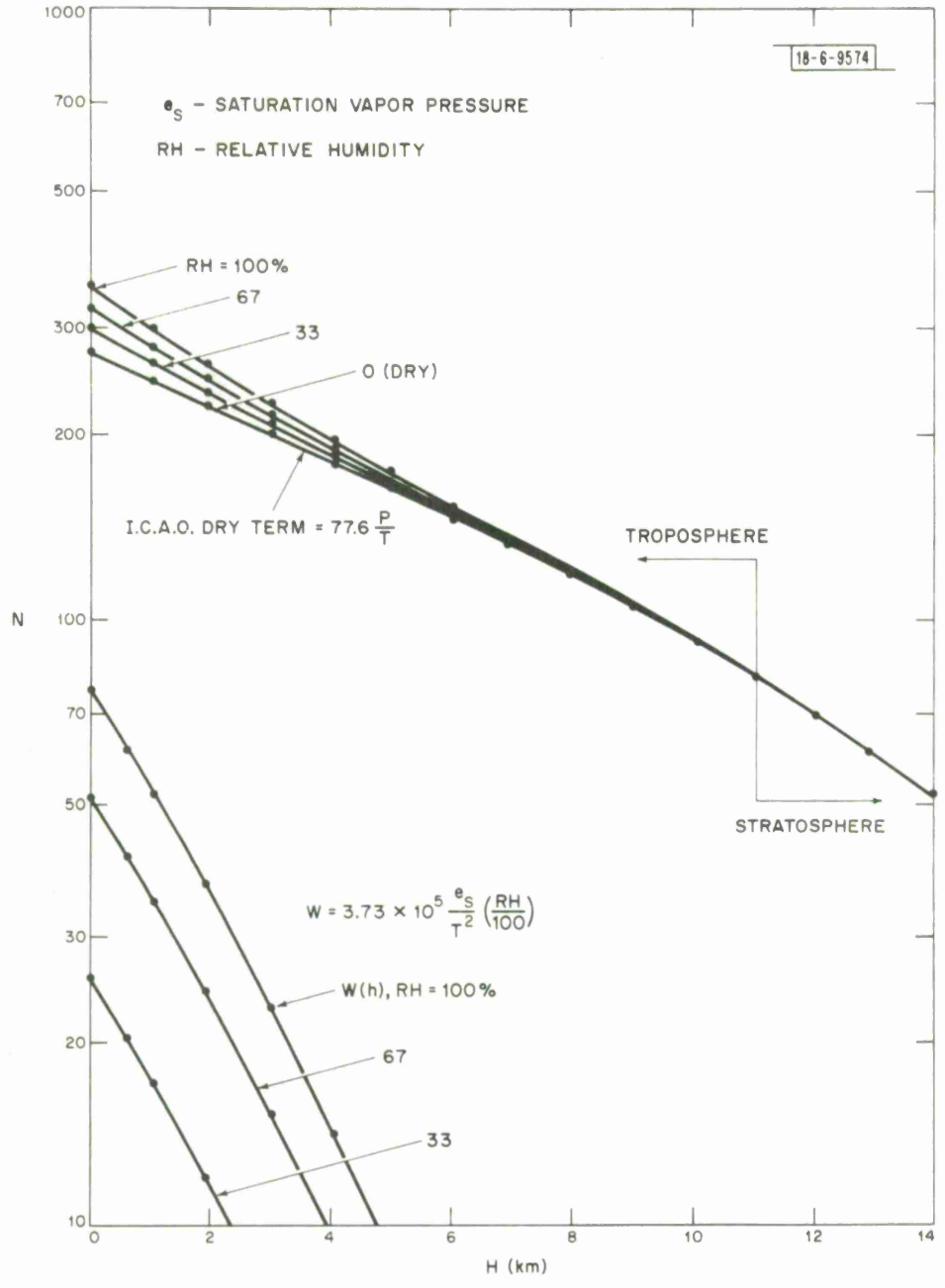

Fig. 2. N distribution for the I.C.A.O. standard atmosphere.

the tropopause region. This layer shows a marked drop in altitude during the winter and a rise in the summer. This points out although we will use a rather simple turbulence model in this report, any more extensive link analysis must consider the larger scale meteorology (in particular the stable and unstable layer distribution).

B. Refraction and Diffraction

Since the atmospheric density decreases systematically with altitude, an oblique radio wave will undergo refraction. The local curvature of the radio ray is given by

$$C = -\frac{1}{\eta}\frac{d\eta}{dh}\cos\epsilon \tag{3}$$

where η and ϵ are local values of the refractive index and the elevation angle. To simplify the geometry of the propagation problem it is customary to straighten out the actual curved path of the radio ray by presenting the straight ray relative to an imaginary earth of radius $k r_e$ where the relative curvature between the ray and earth is maintained

$$\underset{\substack{\text{earth}\\\text{curvature}}}{\frac{1}{r_e}} + \underset{\substack{\text{ray}\\\text{curvature}}}{\frac{1}{\eta}\frac{d\eta}{dh}\cos\epsilon} = \underset{\substack{\text{effective earth}\\\text{curvature}}}{\frac{1}{k r_e}} + \underset{\substack{\text{curvature of}\\\text{straight ray}}}{0} \tag{4}$$

If the "standard atmosphere" gradient

$$\frac{d\eta}{dh} = -\frac{1}{4 r_e}$$

is used then $k = 4/3$ and the effective earth radius is $4/3\ r_e \simeq 8500$ km. The atmosphere in this imaginary earth will have a constant mean η with altitude. Figure 3 [2] shows that for the altitude regime 0 to 17 km, the $(4/3\ r_e)$ approximation gives values of refraction which are less than the actual average bending. Retaining the $(4/3\ r_e)$ approximation will then give us a conservative estimate which is a desirable feature.

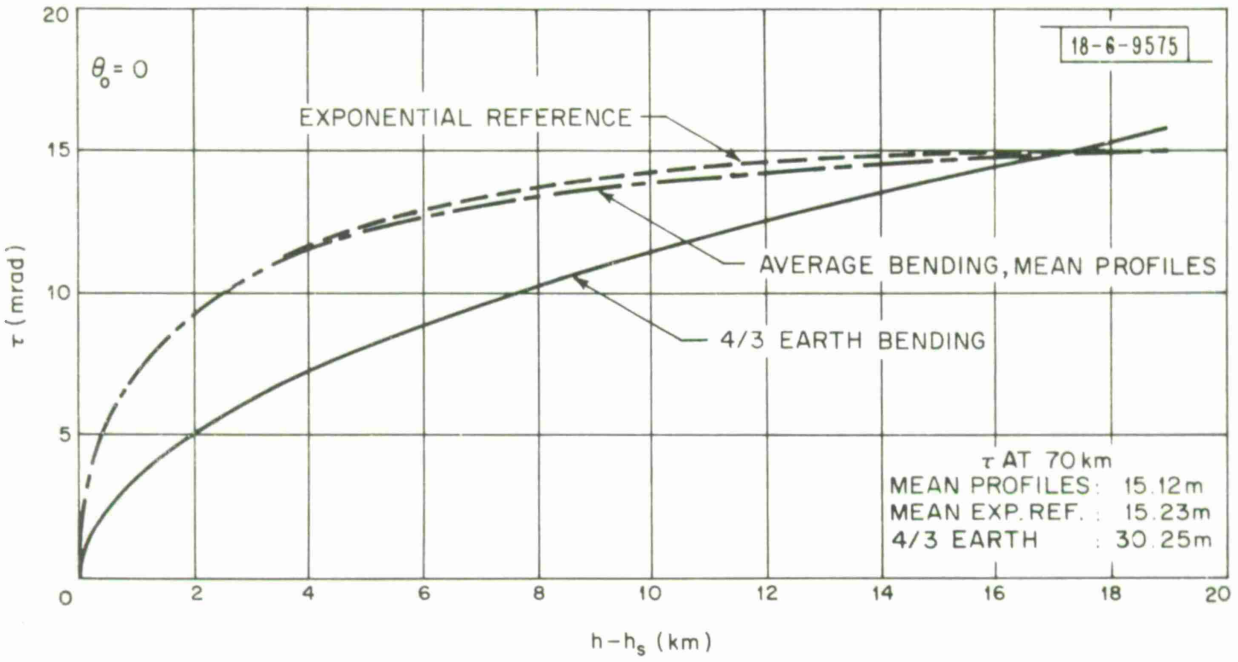

Fig. 3. Refraction corrections.

Two types of diffraction occur in transhorizon propagation; namely diffraction around a smooth spherical surface and knife edge diffraction. For a smooth surface the distance beyond the radio horizon at which the scattered energy and diffracted energy are approximately equal is given by

$$d \simeq 65 \left[\frac{1}{f}\right]^{1/3} \text{ km where } f \text{ is in GHz. For } f \sim 3 \text{ GHz} \tag{5}$$

$$\simeq 21 \text{ km.}$$

Since the horizon distance is of the order of 10 km, it can be safely assumed that the scattered fields will dominate at distances greater than 31 km from the transmitter. At a few hundred kilometers the diffracted fields are entirely negligible. Knife edge diffraction would be significant only if the lower edge of the common volume is directly at or below the top of some obstacle. The section on beam geometry will show that this is not a detectable propagation component.

C. Path Considerations

It is a well known experimental fact that the received scattered power in a troposcatter link decreases rapidly with an increasing scattering angle β (β is defined on Fig. 4). The reason for this is that not only are the theoretical scattering models very β dependent but also the intensity of the turbulence tends to decrease in magnitude for increasingly higher common volumes (that is $\overline{\Delta N^2}$ is altitude dependent which for a bistatic link is impossible to separate from the β dependence). The objective then is to keep the beam as close to the local horizon as possible and at the same time guard against obstacle blockage of the antenna beam.

To see the effect that link distance and obstacles have on β let us first consider a simplified geometry. Assume that the path has a uniform surface elevation of 500 ft. above sea level and moreover that the antenna is placed 20 ft. above this surface (different antenna heights or surface levels can be easily accounted for in most cases by a radial translation). Define

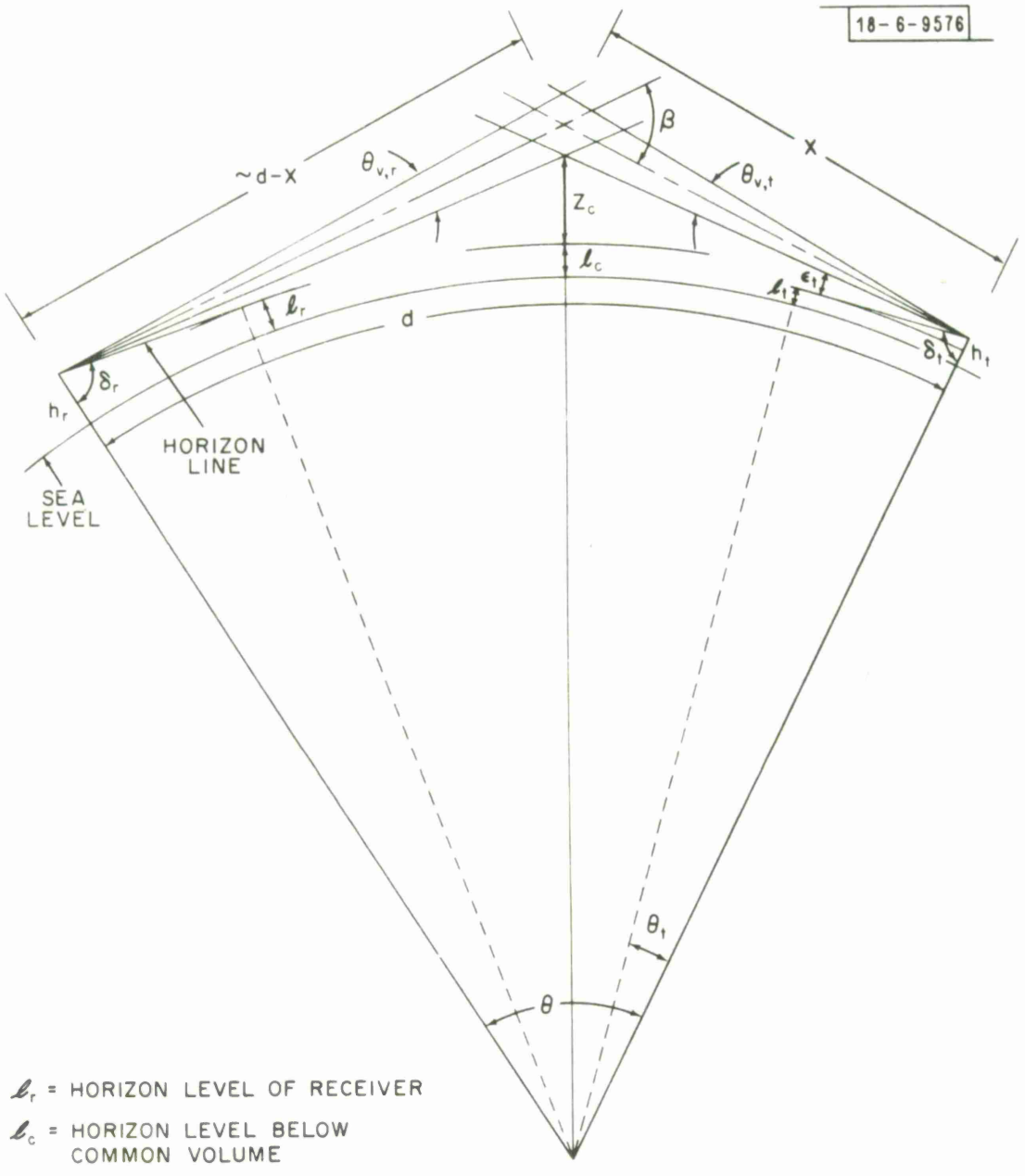

Fig. 4. Link geometry.

the horizon line to be that line passing through the antenna dish center and being tangent to the surface. The elevation angles ϵ are measured with respect to this line. Figure 5 shows the maximum permissible height of obstacles as a function both of elevation angle ϵ and distance from the transmitter (or receiver). Figure 6 shows a similar set of curves which gives the height of the common volume provided both the common volume-receiver (or transmitter) distance and elevation angle ϵ is specified. Here ϵ is understood to be the elevation of the bottom edge of the main antenna lobe. The scattering angle β can be computed from the following set of equations

$$\theta = \left(\frac{180}{\pi}\right) \frac{d}{r_e} \tag{6}$$

$$\delta_t = \sin^{-1}\left(\frac{r_e + l_t}{r_e + h_t}\right), \quad \delta_r = \sin^{-1}\left(\frac{r_e + l_r}{r_e + h_r}\right) \tag{7}$$

$$\beta = \theta + \left(\delta_t + \epsilon_t + \frac{\theta_{v,t}}{2}\right) + \left(\delta_r + \epsilon_r + \frac{\theta_{v,r}}{2}\right) - 180. \tag{8}$$

For the case where the horizon is several km away $\delta_t \simeq \delta_r \simeq 90^\circ$ and

$$\beta \simeq \theta + \left(\epsilon_t + \frac{\theta_{v,t}}{2}\right) + \left(\epsilon_r + \frac{\theta_{v,r}}{2}\right). \tag{9}$$

The normal objective is to make $(\epsilon_r + \epsilon_t)$ as small as possible so that the tropopause is included in the common volume. Communication across mountain ranges is easily possible provided the receiver and transmitter locations are positioned sufficiently far enough away. The standoff distances can be determined from Figs. 5 and 6. For most areas of the United States it is easy to find terminal locations where both ϵ_r and ϵ_t can be made $1/4^\circ$ or less. Accordingly $\epsilon_r = \epsilon_t = 1/4^\circ$ will be used in the calculations. For a troposcatter link of 640 km, the lower edge of the common volume will then be at an approximate altitude of 7 km. This is sufficiently low such that the tropopause layer will be included in the common volume for the

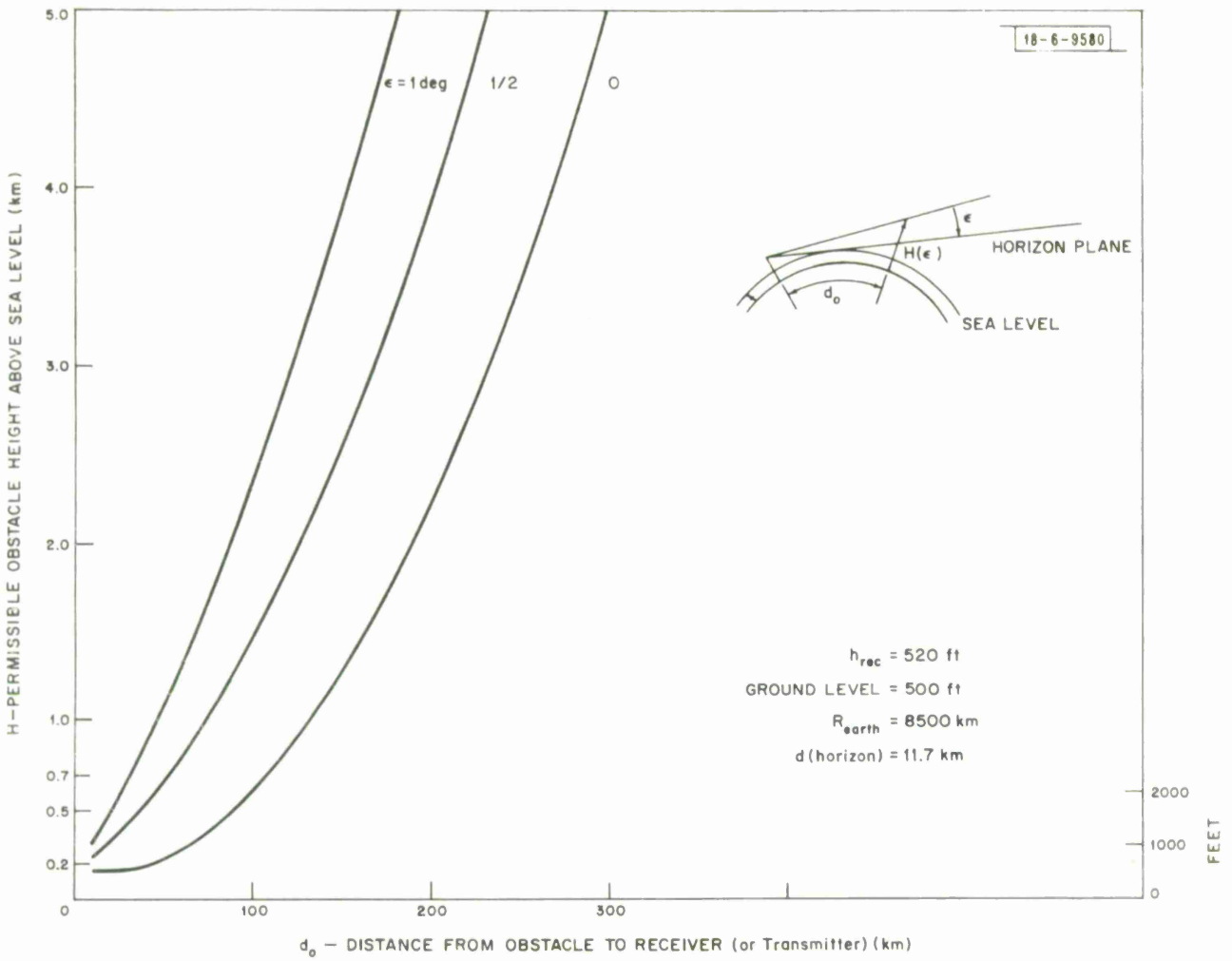

Fig. 5. Permissible obstacle height versus distance from receiver (or transmitter).

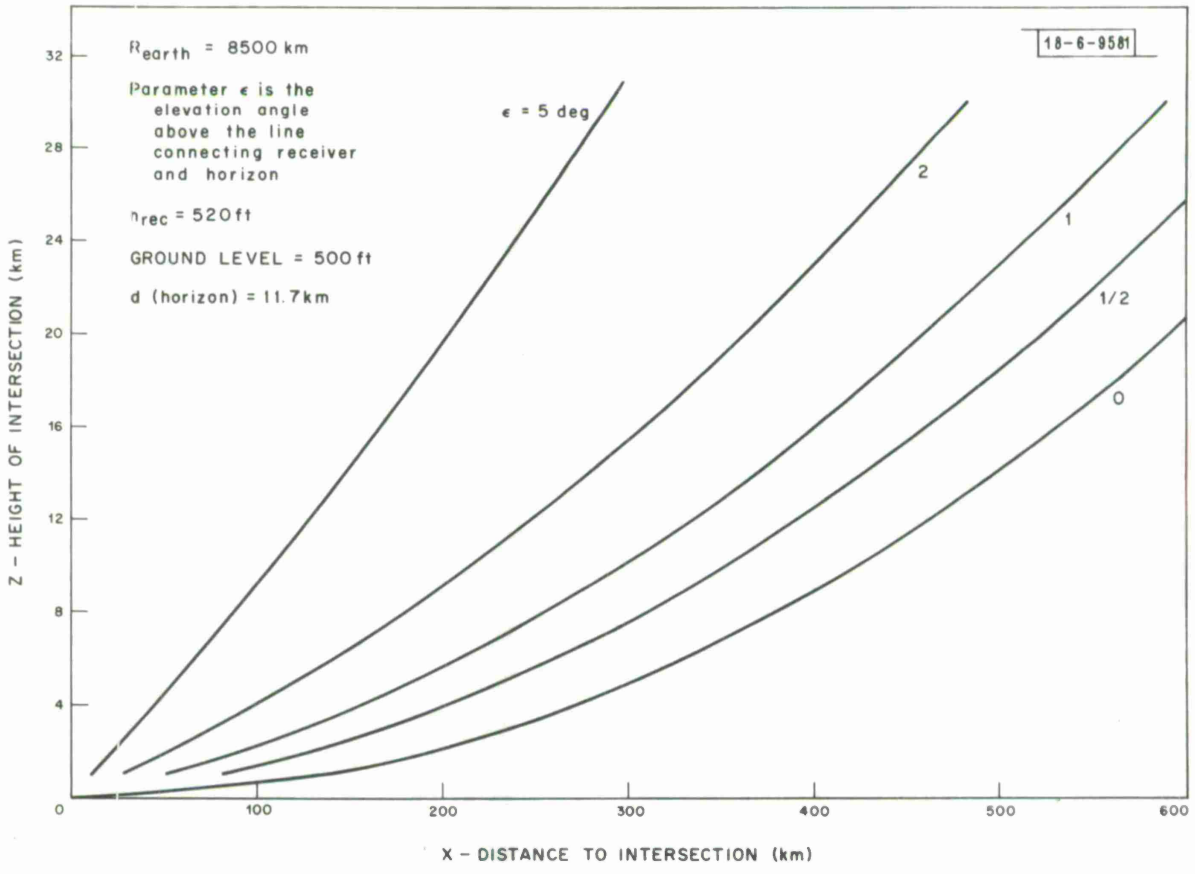

Fig. 6. Common volume altitude.

entire year. The parameters to be used in the sample calculations are then

d	X	$\epsilon_t = \epsilon_r$	$\theta_{v,t} = \theta_{v,r}$	β
640 km	320 (km)	0.25^o	1.5^o	$\sim 6.2^o$

II. System Sizing

A. Method of Calculation of the Required Transmitter Power

One purpose of the report is to provide enough information on the hardware and propagation parameters of a (400 mile) troposcatter communications link so that one can make quick computations for alternative systems. The selection of a system may be constrained by a number of factors external to what we have considered and consequently we have not done an all encompassing parameter study. What we intend to do is to choose an acceptable receiver system, antenna size and beam geometry and to evaluate the average power required for the transmitters. If these power levels are sufficiently low (say 10KW or less) the system will be considered feasible. In computing the required transmitter power level we will account for the various quantities listed in table 1 (and discussed in detail in the identified section).

The formula for minimum transmitter power is listed below. The identification and magnitude of the terms in the formula are discussed in the appropriate sections (all terms in dB). The signs associated with the terms below are consistent with the signs on the figures in the appropriate sections

$$P_T = \underbrace{\left\{N + \frac{E_b}{NT}\right\}}_{\substack{\text{Minimum}\\ \text{Received}\\ \text{Signal}}} - \underbrace{\left\{G_R - L_R + G_T - L_T - L_a\right\}}_{\text{Effective Antenna Gain}} - \underbrace{L_{Pf}}_{\substack{\text{Free}\\ \text{Space}\\ \text{Loss}}} + \underbrace{L_{G,R}}_{\substack{\text{Rain}\\ \&\\ \text{Gas}\\ \text{Atten.}}} - \underbrace{\sigma}_{\substack{\text{Bistatic}\\ \text{Cross}\\ \text{Section}}}$$

$$- 10 \log \underbrace{\frac{d^2}{4\pi |\vec{X}'|^2 |\vec{d} - \vec{X}'|^2}}_{\substack{\text{Distance}\\ \text{Factor of}\\ \text{Bistatic}\\ \text{Radar}}} \qquad (10)$$

A typical computation will be shown in section II-I.

TABLE I

Quantity	Section
Receiver and antenna noise -N = kT_{op}	II-G
Antenna gains $G_T G_R$	II-B
Antenna efficiency $L_T = L_R = 3dB$	
Aperature - to - medium coupling L_a	II-C
Rain and Gaseous Attenuation $L_{R,G}$	II-D
Free Space Attenuation L_{Pf}	II-E
Scattered Power normalized by the Free Space Power P/P_{fs}	II-F
Signal to Noise Ratio $\overline{P}_m/N_o$	II-H

B. Antenna Considerations

Because of the requirements of mobility it is necessary that the antennas be relatively small. If the antenna is say less than 5 meters in diameter one can easily envision systems where any or all of the transmitters and receivers can be made mobile by mounting on trucks. Since troposcatter links require beamwidths of the order of a degree, this requires that the frequency of operation be in the GHz region. Paraboloids are efficient reflectors at these frequencies and are the only antennas considered. The frequency range of interest is from 1 GHz to 8 GHz (the lower limit is constrained by the antenna size and the upper limit by the attenuation due to rain).

In free space the appropriate gain expressions are given by

(a) the directive gain G_D

$$G_D = \frac{\text{max rad. intensity}}{\text{average rad. intensity}}$$ If θ_H, θ_V are the half-power beamwidths in two orthogonal plans the directive gain can be approximated by

$$G_D = \frac{41253}{\theta_H \theta_V} \quad (\theta_H, \theta_V \text{ are in degrees}) \tag{11}$$

(b) the power gain G

$$G = \frac{\text{max rad. intensity}}{\text{rad. int. from lossless isotropic source with same power input}}$$

(c) The radiation efficiency factor ρ_r

$$\rho_r \equiv \frac{G}{G_D} < 1 \tag{12}$$

(d) Effective aperature A_e and antenna aperature efficiency

$$G = \frac{4\pi A_e}{\lambda^2} = \frac{4\pi \rho_a A}{\lambda^2} \qquad \text{A is physical size of antenna.} \quad (13)$$

Combining equations 11, 12 and 13 gives

$$\theta_H \theta_V = 41253 \frac{\lambda^2 \rho_r}{4\pi A \rho_a} \qquad \text{For the paraboloid of diameter D}$$

the approximate mainlobe beamwidth is

$$\theta = \sqrt{\theta_H \theta_V} = \sqrt{41253} \sqrt{\frac{\rho_r}{\rho_a}} \left(\frac{\lambda}{\pi D}\right) \text{ [degrees]} \qquad (14)$$

Figure 7 gives the beamwidth as a function of frequency with the diameter of the paraboloid (D) as a parameter. The antenna gain divided by the aperature efficiency is shown in Fig. 8.

C. Aperture-to-Medium Coupling Loss

The theoretical antenna gain expressions just described presuppose that the incident wave is an ordinary plane wave. However, in scatter propagation the individuals scatters in the common volume produce a wave at the receiving antenna which is not planar and hence the full gain of the antenna will not be realized. The incoherence of the wave front causes an effective gain reduction which is greater for the large antenna than for the small antenna. There exists no simple relationship which accurately gives the coupling loss in terms of the antenna parameters and geometry alone. Hence we must estimate this loss by comparison of the proposed antenna parameters with existing experimental estimates of aperture-to-medium coupling losses. Yeh [3] has collected a large number of experimental estimates and plotted them versus the parameter $\beta/\sqrt{\theta_V \theta_H}$. (Fig. 9) For a typical case in the GHz region for the 400 mile link we have

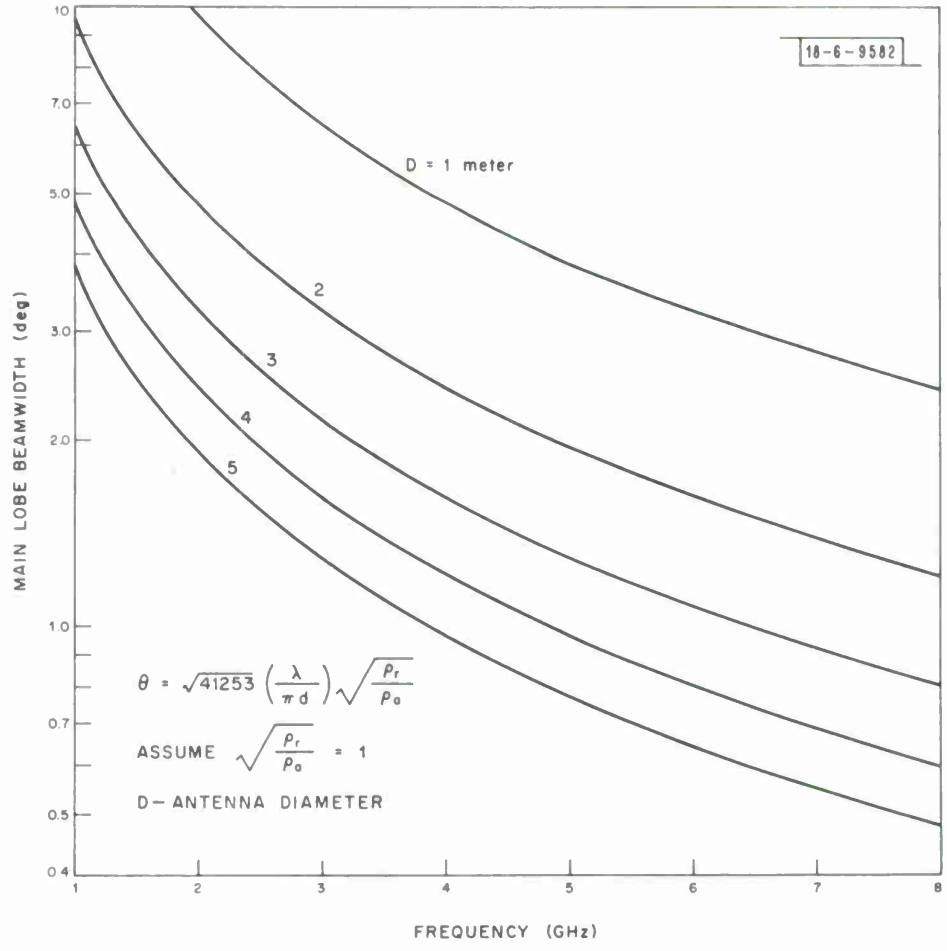

Fig. 7. Beamwidth versus frequency.

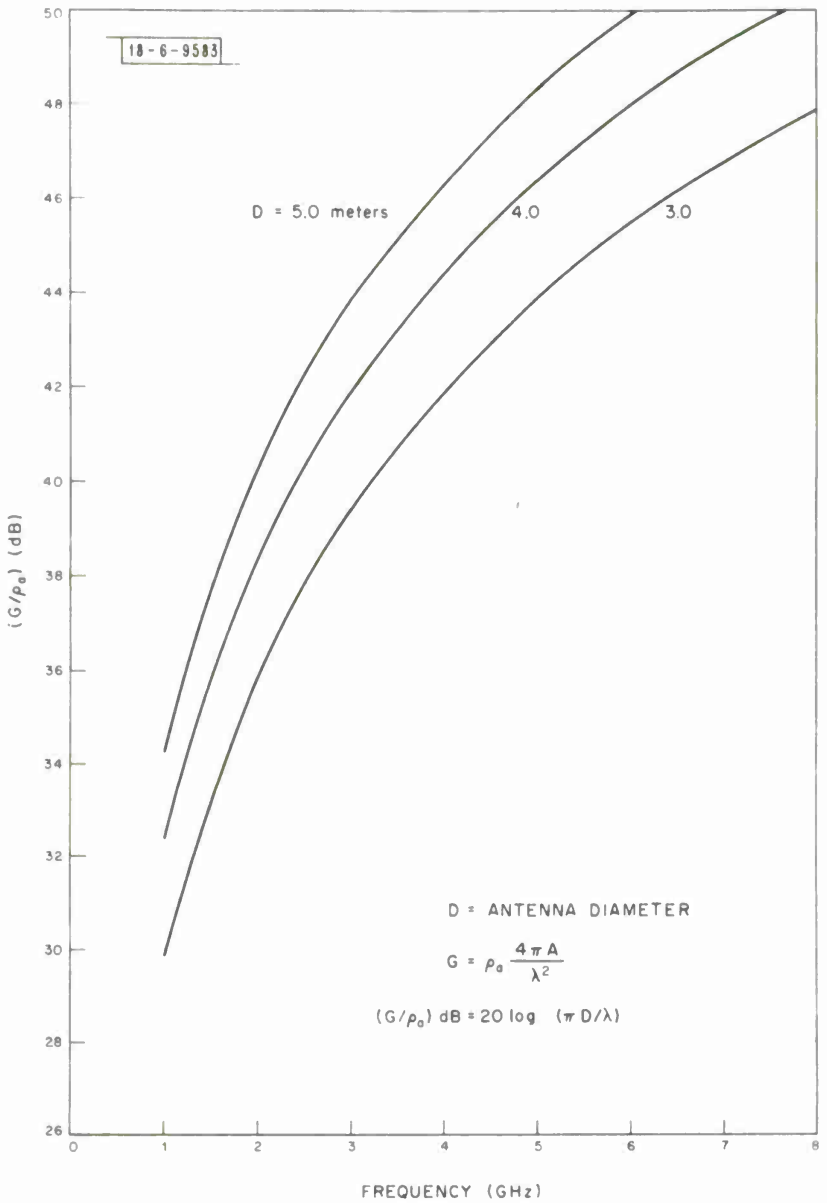

Fig. 8. Antenna gain versus frequency.

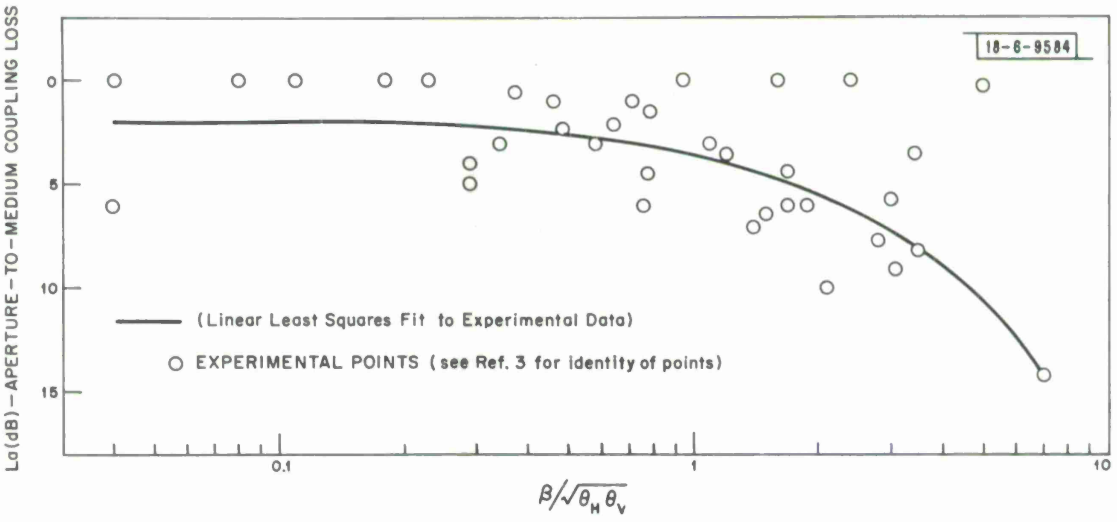

Fig. 9. Aperture-to-medium coupling loss.

$$\frac{\beta}{\sqrt{\theta_V \theta_H}} = \frac{6.2^\circ}{\sqrt{(1.5)^\circ (1.5^\circ)}} \simeq 4.1^\circ$$

This gives an aperture-to-medium coupling loss of about 9.0dB which is probably slightly on the conservative side.

D. Rain and Gaseous Absorption Loss

In the GHz region, attenuation due to rain and the gaseous absorption can become significant. Fig. 10(Bean [1]) shows the total attenuation due to these two sources as a function of frequency. The magnitude of the values of attenuation will be less than the curves 99% of the time. The 400 mile values can be easily interpolated from the two curves for 300 mile and 1000 mile path lengths. For example at 4GHz the total path attenuation is about 4.5 dB. The rapidly increasing attenuation with frequency is the fact that restricted our investigation to frequencies less than 8GHz.

E. Free-Space Attenuation

In scatter theory the received power is usually normalized by the power that would be received over a line-of-sight path. For lossless propagation the free space power is given by

$$P_{fs} = P_T G_T G_R \frac{\lambda^2}{16\pi^2 d} \tag{15}$$

The basic propagation attenuation in free space is defined by

$$L_{Pf} \equiv \frac{P_{fs}}{P_T G_T G_R} = \left(\frac{\lambda}{4\pi d}\right)^2 \tag{16}$$

L_{pf} is plotted in Fig. 11 with d as a parameter. Now the theoretical gain product should be modified by the aperture-to-medium coupling loss La.

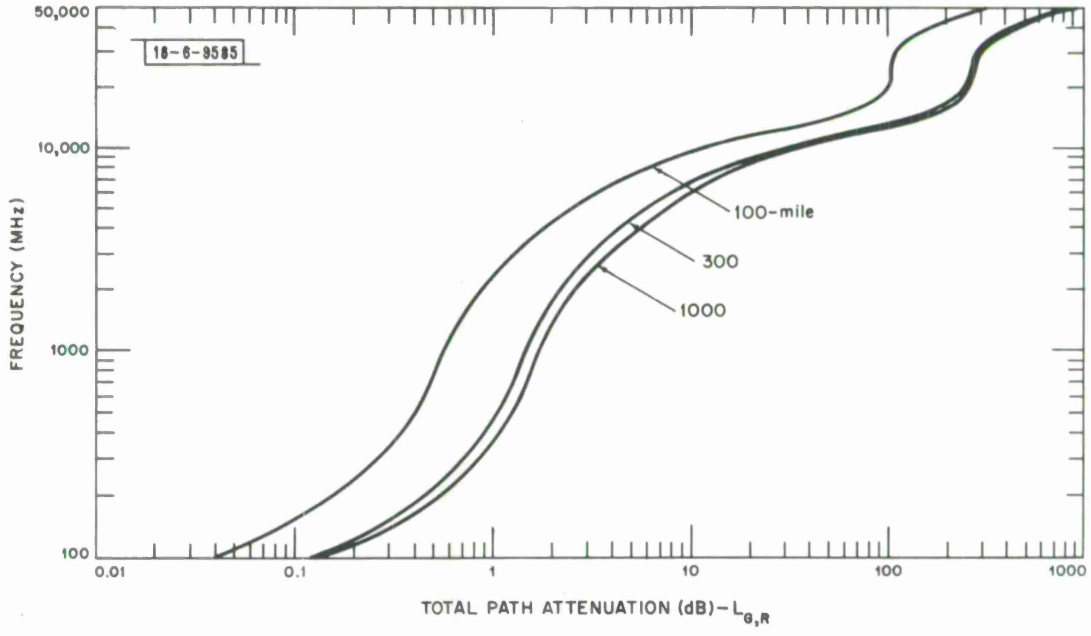

Fig. 10. Combined rain and gaseous absorption (1% exceedance values).

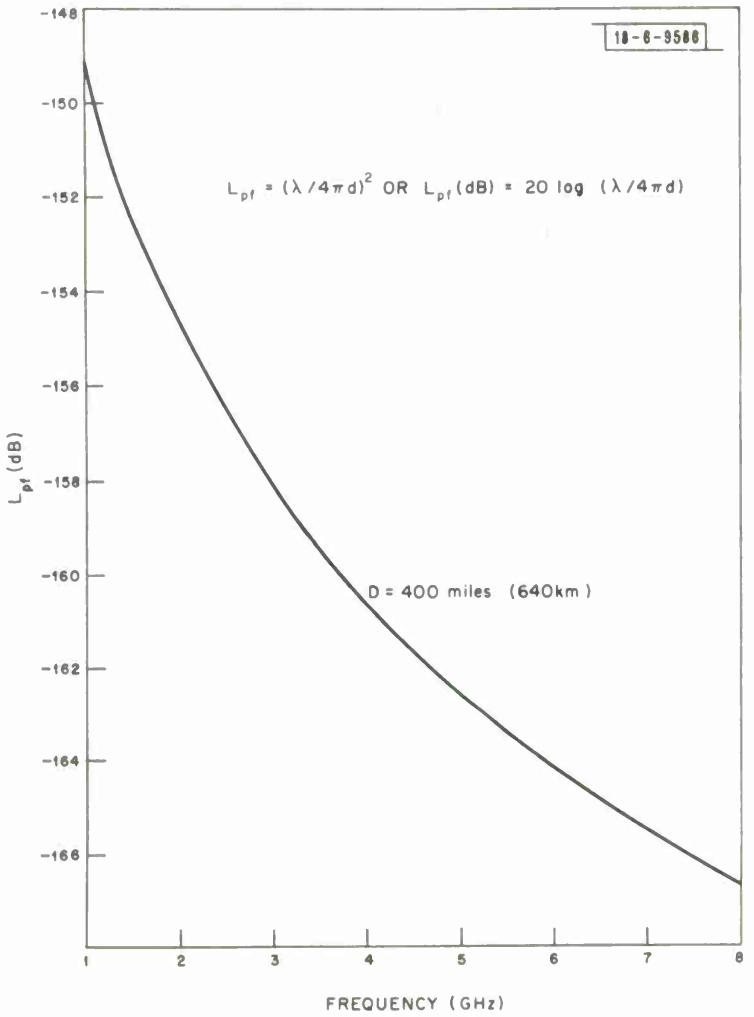

Fig. 11. Free space attenuation.

The free space power is then given by

$$P_{fs}[dB] = P_T - L_{Pf} + \left\{G_T + G_R - L_a\right\} \text{ (all terms in dB)} \quad (17)$$

F. Scattering Theory

In a previous section we have accounted for refractive corrections and excluded diffraction as being important. 'Scattering' is often used as an all inclusive name in transhorizon propagation to describe any energy which leaves the common volume region in a direction different from the axis of the transmitter beam. For long distance links we are fortunate in that only one mode (the usual inhomogeity scattering)dominates.

Various physical models for transhorizon propagation were developed during the 1950's.[5] During that time there was major debate on whether the appropriate mechanism was specular reflection from elevated layers or scattering from the refractive index fluctuations caused by the atmospheric turbulance. Gradually the adherents of the scattering theory became more prevalent even though no single mathematical scattering model consistently agreed with the experimental results. In the early sixties extensive experimental work by the French (see DuCastel [4]) revealed that the received signal contained a mixture of scattered in addition to diffuse and specularly reflected energy. Since then the main effort has been to obtain a viable syntheses of these diverse theories. For long distance propagation (if we neglect anomalous effects which are not too uncommon) the recent tendency has been to describe the physical process in terms of a standard scattering model and to include the effects of any layering in the autocorrelation coefficient of the refractive index variations. This will be the approach used here.

The fact that energy is reflected/scattered from layered regions is now well established. For long distance transhorizon propagation the layers at the tropopause level provide a good scattering region (this is certainly true for the 400 mile links considered in this report.) To a lesser extent layers

in the stratosphere also contribute to the scattered return.

In Appendix A we have outlined the derivation of the equation for the average received power normalized by the free space received power (equation a-20). The electrodynamics in this derivation are complex but are relatively straight forward requiring few physical assumptions. We have, however, been forced to assume local homogeneity in the statistics of the refractive index fluctuations. This barely tolerable assumption is made because the alternative leads to a prohibitively difficult problem. If the beams are very narrow this is however a reasonable assumption to make. The remaining difficulty is to specify the form of the spectrum ($\Phi_n(K)$) of the refractive index fluctuations. Many investigators over the years have postulated various mathematical models for $\Phi_n(K)$. Usually these models took the form of $\Phi_n(K) \approx K^{-m}$ where m is a fixed constant. However none of these models have been universally accepted because the experimental evidence often seemed contradictory. It was soon realized that for physical reasons the refractive index spectrum had a variable wavelength dependence.[6] Fig. 12 * shows such a spectrum broken up into three regions each with a different exponential dependence. At present the most widely used exponent is $m = -11/3$ which refers to the inertial subrange. It should be noted that this dependence was first arrived at by Kolmogorov in 1941 on the basis of a simple similarity analysis of the turbulence. (see Tartarski [7] and Bachelor [8] for details). In most of the cases where experimental evidence seems to show that the "11/3" dependence law "fails" it is often because the value of $K(= 2k \sin \beta/2)$ for that particular experiment lies outside the inertial subrange.

*Inasmuch as we have assumed that C_n^2 is dependent on position we will plot $\int_{\vec{V}\gamma} \Phi(K, \gamma) d\vec{\gamma}$ rather than $\Phi(K, \gamma)$ since there exists numerical values derived for the former but not the latter quantity.

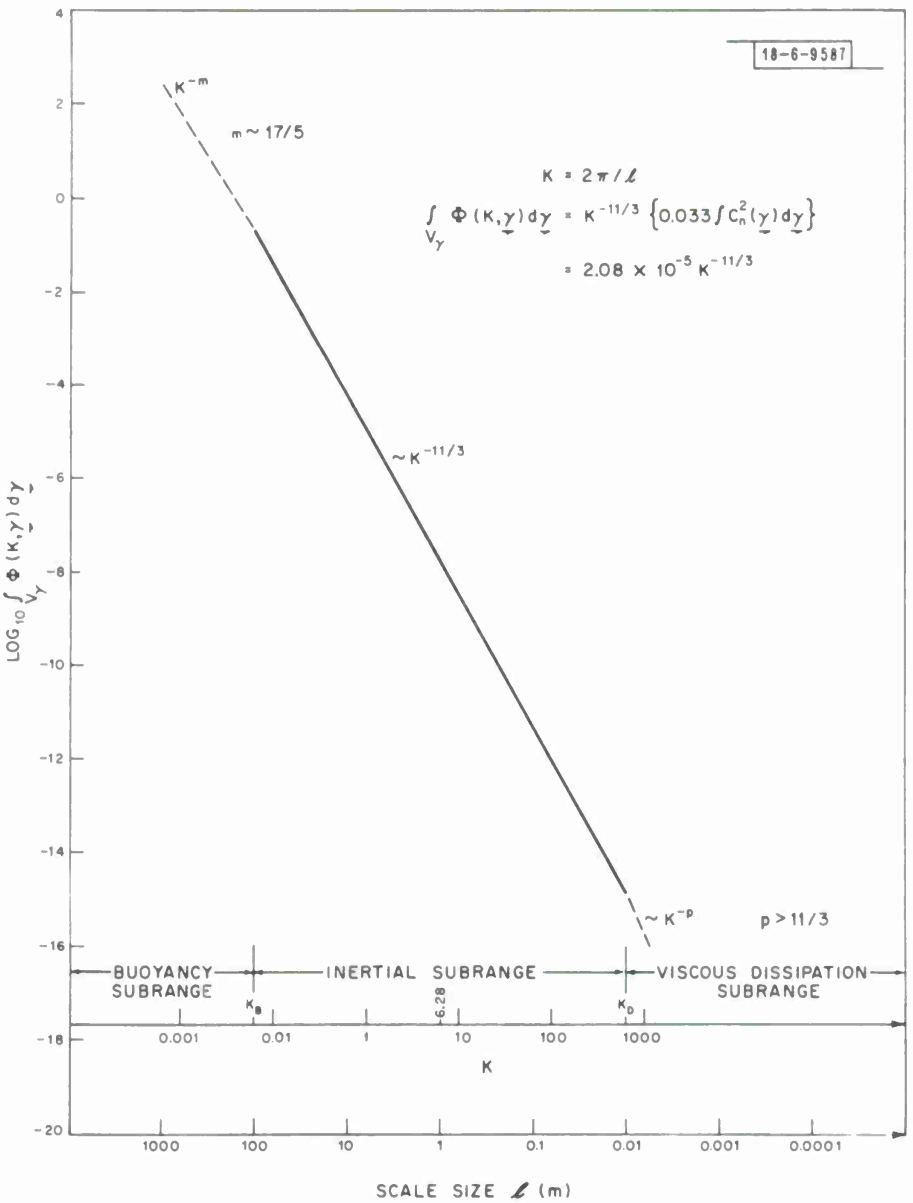

Fig. 12. $\text{Log}_{10} \int_{V_\gamma} \Phi(K, \underset{\rightarrow}{\gamma})\, d\underset{\rightarrow}{\gamma}$ versus scale size ℓ.

This is particularly true for the longer wavelength and shorter path links where both k and β are smaller (this means that the characteristic eddy size $l = \frac{2\pi}{K}$ is typical of the buoyancy subrange which has a different value of n). Most of the common troposcatter links fall in this category and hence this is to a large part the reason why the standard scattering theories were not well accepted. For the GHz range we are usually in the inertial range. For example if we take f = 3GHz and $\beta = 6.2^{o}$ the characteristic (scale) size is

$$l = \frac{2\pi}{K} = \frac{\lambda}{2 \sin \beta/2} = .91 \text{ meters} \qquad (18)$$

This value of l is well within the inertial subrange and hence the "11/3" law should be appropriate. Tartarski [7] gives the spectrum as

$$\Phi_n(K) = (.033) C_n^2 K^{-11/3} \qquad (19)$$

When this is substituted into equation a-21 the bistatic scattering cross section is

$$\sigma = (.384)(\sin^2 \chi)\lambda^{-1/3} (\sin \frac{\beta}{2})^{-11/3} \int_{V_\gamma} C_n^2(\gamma) d\gamma \qquad (20)$$

The geometry and frequency being specified it only remains to determine the volume integral $\int_{V_\gamma} C_n^2(\gamma) d\gamma$. This of course can only be determined experimentally.

Crane [9] has recently undertaken an experiment which has given some quantitative estimates to the volume integral $\int_{V_\gamma} C_n^2(\gamma) d\gamma$. The entire experiment will be first described in moderate detail since the parameters are very similar to the scatter links we are proposing and accordingly provides the feasibility for undertaking our troposcatter link. His experiment utilizes both monostatic and bistatic scattering techniques. The narrow beam Millstone L band radar

was used to determine the spatial distribution of the layers through back scattering cross section measurements. Then an X-band forward scatter link (between Wallops Island, Va. and Westford, Mass.) provided the normal transhorizon data. The important parameters of the X-band forward scatter link are

(a) frequency $\cong$ 7.7GHz

(b) c.w. power $\simeq$ 1kw

(c) minimum detectable signal = -190dBw (signal levels ranged from -174dBw to -190dBw)

(d) transmitter antenna has 6ft. diameter and varied in elevation while the receiver antenna had a 60ft. diameter with a ($.8^{o}$) elevation angle.

(e) path length = 628km (390 miles)

The significant results of the experiment were

(a) Layers were always detected near (and above) the tropopause

(b) This layer showed a relatively uniform backscattering cross section

(c) Turbulent layers were detected up to 22km (well into the stratosphere)

(d) The signal in the forward scatter link in terms of its scattering angle dependence was consistent with the well known "11/3" law of turbulent scattering.

(e) From radiosonde data and the radar data, estimates of C_n^2 for the layers were made. Because of the resolution of the L band pulse length only ($C_n^2 l_t$) could be determined (where l_t is the layer thickness). A typical value of ($C_n^2 l_t$) is $10^{-12}(m^{1/3})$. Then $\int_{V_\gamma} C_n^2(\gamma)d\gamma \simeq 10^{-12} A_t [m]^{7/3}$ where A_t is the horizontal layer area limited by the common volume.

If we consider the geometry appropiate to our problem, the area limited by the common volume (assuming that the tropopause is at 10km) is given by (see Fig. 19 in Appendix B)

$$A = \frac{(\Delta Z) D \hat{\theta}_H}{2 \tan(\beta/2)} \simeq \frac{(10-6.5)650(1.5)^{\Pi}}{2 \tan(2.7) \quad (180)} \times 10^6 = 6.26 \times 10^8 \, m^2$$

and hence the volume integral is computed as

$$\int_{V_\gamma} C_n^2(\gamma) \sim 6.3 \times 10^{-4} \, [m^{7/3}]$$

Therefore from equation 20 we have

$$\sigma \simeq (2.41 \times 10^{-4}) (\sin^2 \chi) \lambda^{-1/3} (\sin \frac{\beta}{2})^{-11/3} \qquad (21)$$

We will ignore the small polarization effect (since $82^\circ < \chi \leq 90^\circ$) and compute σ as a function of λ for a few different values of β. This is seen in Fig. 13

We are attempting to compute $P(d)/P_{fs}$. This can be computed with the use of equation a-22.

$$\overline{P(d)}/P_{fs} = \sigma \, [dB] + 10 \log_{10} \frac{d^2}{(4\pi) |\underset{\rightarrow}{X'}|^2 |\underset{\rightarrow}{d}-\underset{\rightarrow}{X'}|^2} \qquad (22)$$

If we assume d=650km and $|X'| = |\underset{\rightarrow}{d}-\underset{\rightarrow}{x}'| = 325$km then

$$10 \log \frac{d^2}{(4\pi) |\underset{\rightarrow}{X'}|^2 |\underset{\rightarrow}{d}-\underset{\rightarrow}{x}'|^2} = -115.2 dB$$

and

$$\overline{P}(d)/\overline{P}_{fs} = \sigma - 115.2$$

As an example at f = 3GHz, $\beta = 6.2^\circ$ Fig. 13 gives a value of 13.6dB and hence $\overline{P}(d)/P_{fs} = -101.6$dB. Figure 14 shows some experimental results collected for different links by N. B. S. Our value of $\overline{P}(d)/P_{fs}$ would seem to be consistent with this data.

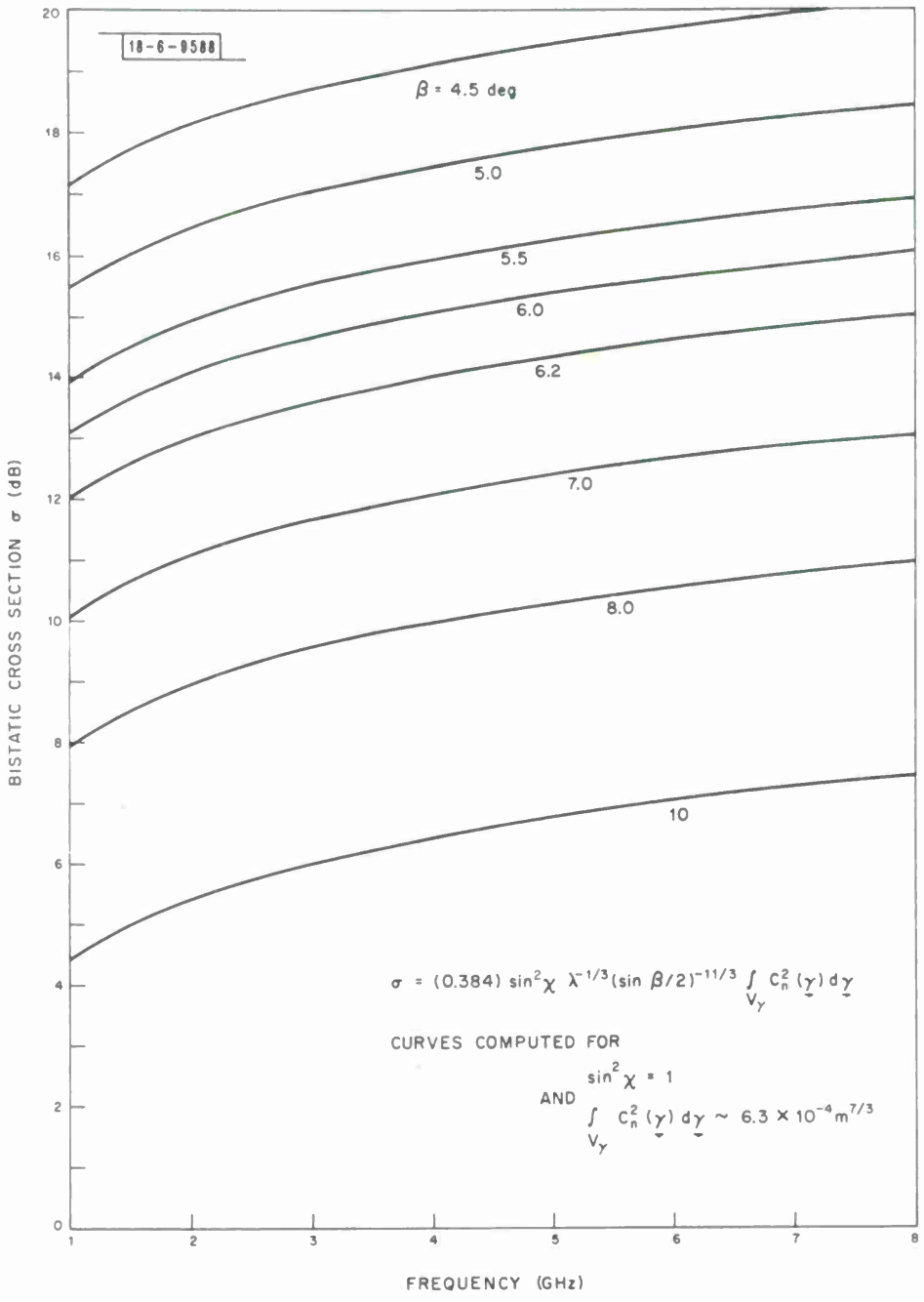

Fig. 13. Scattering cross section σ versus frequency.

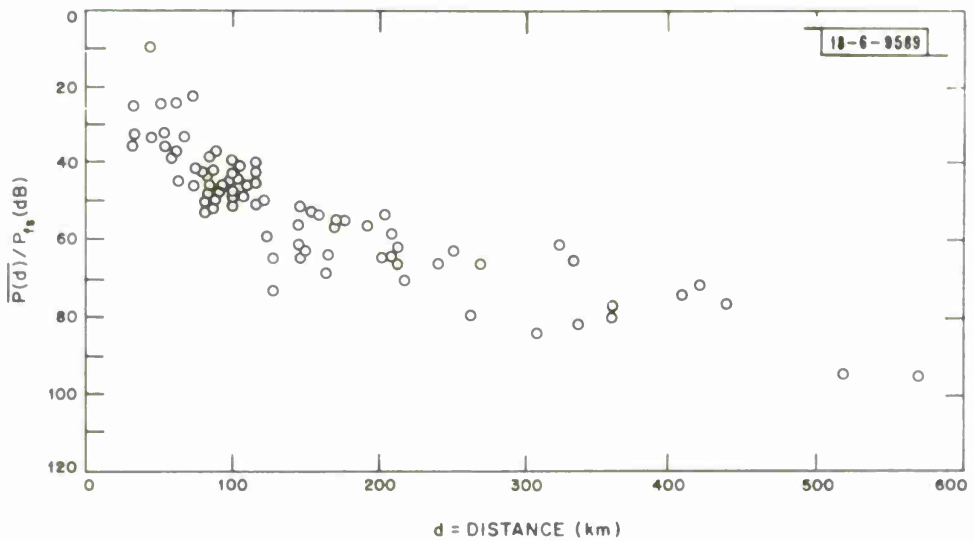

Fig. 14. Spread of experimental results.

G. Noise Considerations

Noise sources are often classified as originating extra-terrestially, terrestially and internally to the receiver system. In the GHz region cosmic noise is insignificant as compared to the receiver noise. Likewise man-made and lightning noise can be ignored in this frequency regime. Unfortunately we cannot ignore the earth's radiation since the main lobe is almost tangential to the horizon and the side lobes illuminate the earth's surface. Moreover because of the effects of aperature blockage by the antenna feeds it is seldom possible to get the nearest sidelobes down more than 15dB relative to the main lobe. The side lobes illuminating the earth (whose $T_b \sim 300^{\circ}K$) then contribute to the effective antenna temperature.

Let us estimate the effective antenna temperature for the proposed beam geometry ($\varepsilon \sim 0^{\circ}$. The effective antenna temperature is computed from

$$T_a = \frac{1}{4\pi} \iint G(\theta, \varphi) T_b(\theta, \varphi) \sin\theta \, d\theta \, d\varphi \qquad (23)$$

where T_b is the brightness temperature of the Rayleigh-Jeans law. From Fig. 15 it is seen that when the antenna beam is tangent to the earth's surface the brightness temperature in this direction is about $120^{\circ}K$ (for the GHz region considered. Now if we are using narrow beam high gain antennas ($\theta \sim 1.5^{\circ}$, $G\max \simeq 10,000$), then the <u>average gain</u> in directions other than the main lobe can be crudely approximated by

$$G_{AV} \sim \frac{2}{1+\cos\theta/2} - \frac{G\max(1-\cos\theta/2)}{(1+\cos\theta/2)} \sim (.56)$$

Since about 1/2 of the sidelobe structure looks at the ground (at $T_G = 300^{\circ}K$) and the other 1/2 looks at the sky ($T_{SKY, AV} \sim 100^{\circ}K$) we can get an approximate antenna temperature of

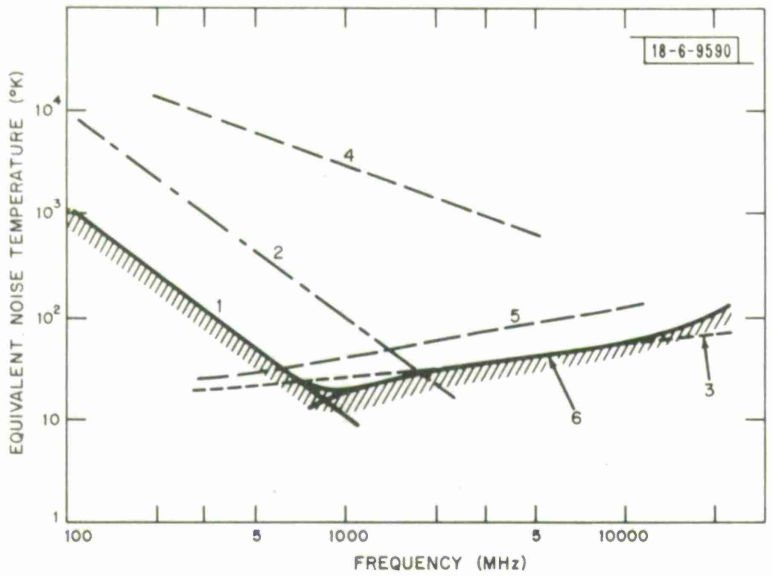

(a)

(b)

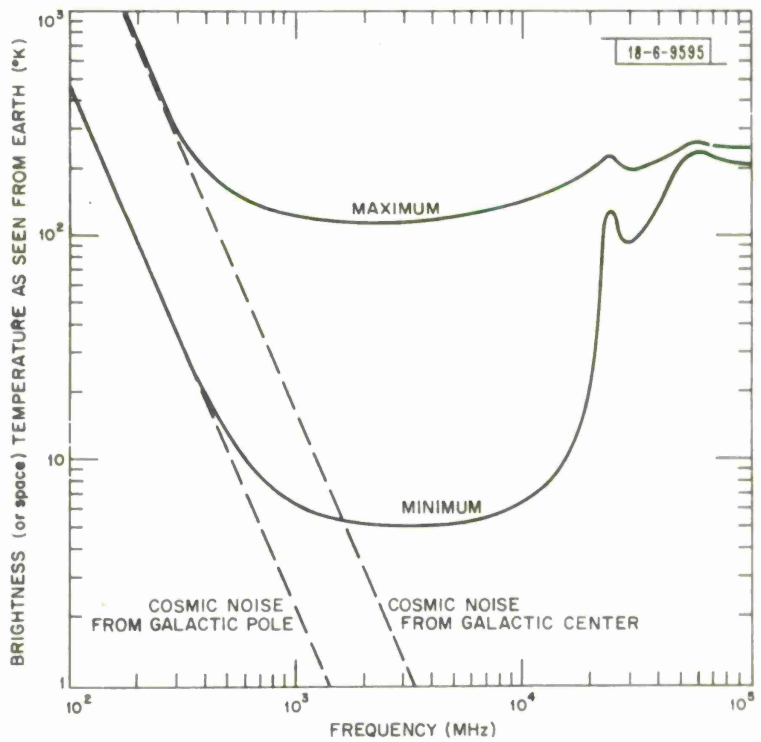

Fig. 15. Noise levels.

$$T_a \simeq \frac{1}{4\pi}\left(2\pi G_{AV} T_G + 2\pi G_{AV} T_{SKY,AV} + G\max\,(\pi(\theta/2)^2) T_{HOR}\right)$$

$$\simeq (.28)\, T_G + (.28)\, T_{SKY,AV} + .44\, T_{HOR} \qquad (24)$$

$$\simeq (.28)\,(300^\circ) + (.28)\,(100^\circ) + (.44)\,(120^\circ)$$

$$\simeq 164^\circ K$$

Since the antenna temperature is relatively high (by radio astronomy standards) it is not worthwhile employing an ultra low noise receiver system. Instead we choose as the receiver an uncooled parametric amplifier with an effective noise temperature of $200^\circ K$. The total operating noise temperature is then

$$T_{op} = T_A + T_{eff} = 364^\circ$$

The noise power per 1Hz bandwidth is then given by

$$N = k\, T_{op} \text{ and in terms of dB this is} \qquad (25)$$

$$N = -204 + 10\log_{10}\left(\frac{364^\circ}{290^\circ}\right) \simeq -203 \text{ dB/Hz}$$

The next factor one must consider is the bandwidth of the individual receiver channels. The required bandwidth is dependent on several factors which will be examined in the following section.

H. Signal to Noise Ratio and Bandwidth Considerations

There are many factors which must be taken into account before specifying the signal to noise ratio which must be known in order to determine the transmitter power level. Let us investigate in turn the transmitter, the

propagation medium and the receiver.

Transmitter - It is initially assumed that the bandwidth for each of the receiver channels is 3KC (this will be justified later in the section). The transmitter will operate in a FSK mode (with $2n_p$ possible frequencies, n_p being the number of chips per bit of information). Transmitter tubes which are self oscillators (like the magnetron) usually do not have the long term or short term frequency stability necessary to keep the transmitted frequency within the required passband of the individual receivers. Accordingly we specify that a klystron with external (crystal controlled) oscillator with stabilities of 1 part in 10^8 be used. This gives a maximum frequency deviation $\sim \pm 30$Hz at 3GHz. ($2n_p$ such oscillators will be needed in the transmitter as well as in the receiver).

Propagation Path - For the path geometry considered the following facts are cogent

(a) For path distances greater than 300 miles, the short term statistics (less than 1 hr.) reveal that the received signal envelope is very close to being Rayleigh distributed and the phase has a uniform distribution.

(b) The differences in path length for any two rays is extremely small. For example with $\beta \sim 6.2^\circ$, $\theta \sim 1.5^\circ$ and D = 650 km equation b-4 gives a path difference of .92 km which corresponds to a 3μsec delay. This means that the receiver integration times can safely be brought down to less than a tenth of a millisecond if desired. The channel bandwidth depends indirectly on these differences in path length. The small delay suggests the bandwidth may be of the order of a MHz. (Unfortunately experimental attempts to determine the bandwidth of tropospheric channels have been very sparse and experimentation in this area should be undertaken.)

(c) The doppler frequency due to motion of the atmospheric irregularities cause band spreading at most of only of the order of tens of Hz and accordingly can be neglected as far as band spreading is concerned.(The doppler shifts

do however effect fading) The maximum doppler shift Δf_d is computed from

$$f_d = f \frac{1 + \frac{u}{c} \sin \frac{\beta}{2}}{1 - \frac{u}{c} \sin \frac{\beta}{2}} \qquad (26)$$

If $\beta \simeq 6.2^o$ and $f \sim 3$GHz

$\Delta f_d = f_d - f \simeq (.54)u$ Hz where u is the irregularity velocity in m/sec.

(d) The fading rates are high both due to the long distance and high frequency. The mean fading time is of the order of 0.1 sec. or less.

Receiver- The receiver is of course the key to the feasibility of this troposcatter system. Let us assume that we are going to operate in a non coherent FSK mode with a binary bit transmission rate of 1000 bits/sec. Let us assume further that at present we are restricted to frequency and time diversity. We will propose the following receiver system so as to obtain a sizing of the transmitter power (alternate and more detailed specifications of receiver systems will be examined in a future report). Each bit is constructed of three frequency chips of duration 1/3 millisec. This specifies 6 possible transmission frequencies. The received signals at the three frequencies that constitute a bit are assumed to be statistically independent. This requires that the three frequencies be separated by the propagation channel bandwidth mentioned above. Let us assume that we have an optimum (frequency) diversity combining system based on Rayleight envelope statistics. A typical receiver channel is shown in Fig. 16. Zero or one decisions are based on a comparison of the values of the y_i values. [12]. The probability of error- versus the energy per bit to noise ratio is shown in Fig. 17 with the number of chips per bit as a parameter. Then for a bit error probability of 10^{-3} and for 3 chips per bit the ratio $E/N = (\sim 17.4$ dB).

The signal to noise ratio is given $\frac{P_m}{N} = \frac{E}{NT}$ where T is the bit duration (1 millisec.) Thus the signal to noise ratio in dB is

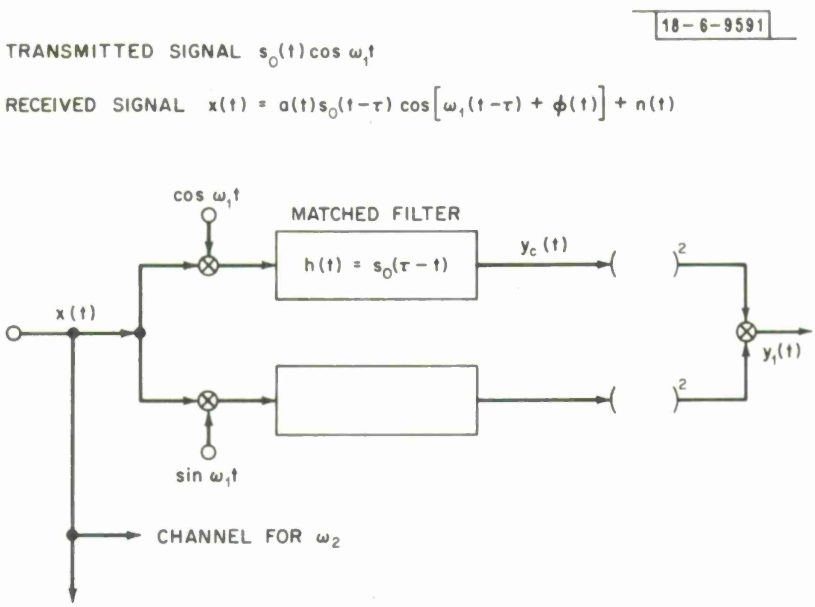

Fig. 16. Typical receiver channel.

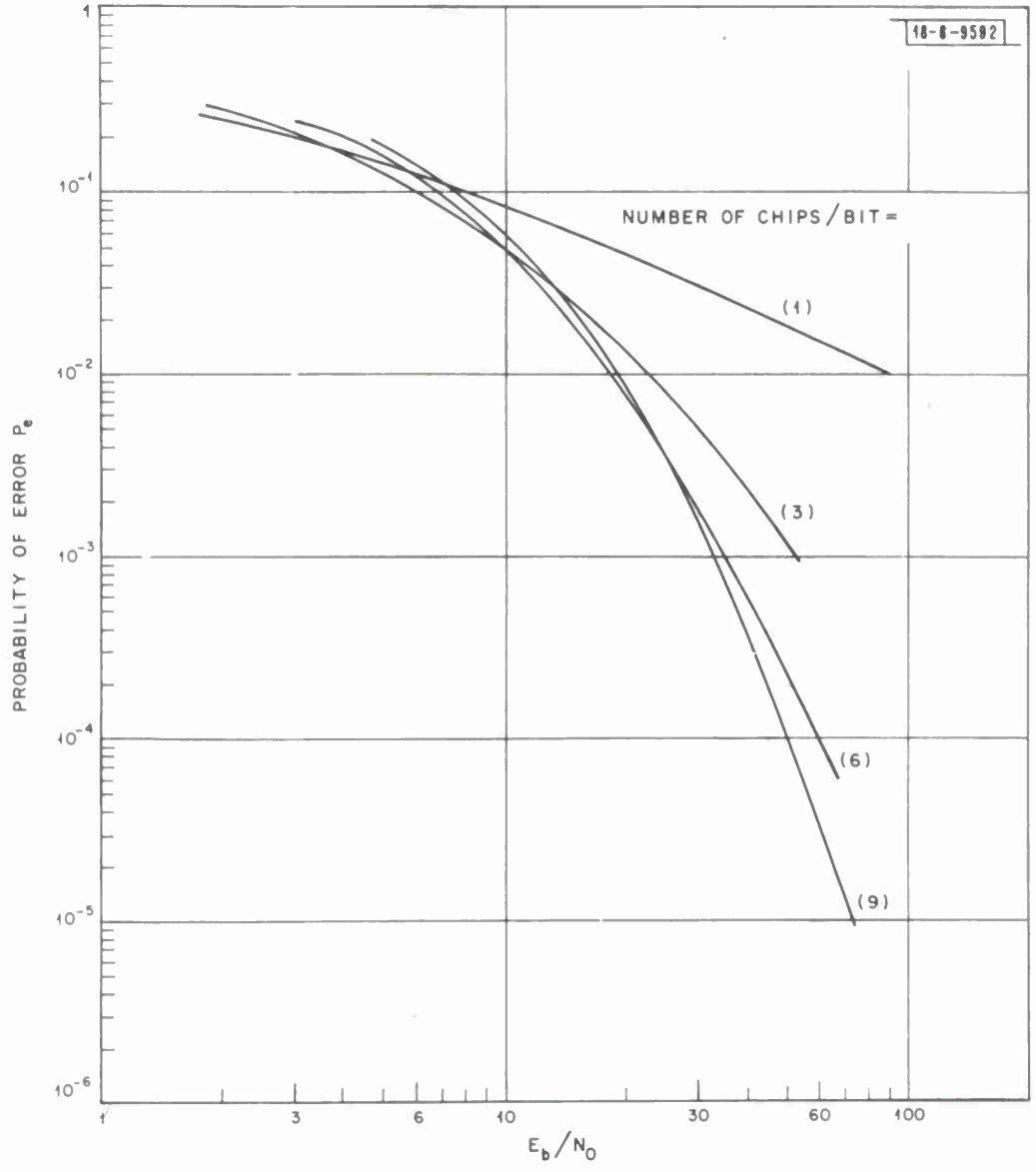

Fig. 17. Binary system with optimum diversity combining.

$$\frac{\bar{P}_m}{N} = 17.4 + 30 = 47.4 \text{ dB}$$

The minimum average received signal level for this receiver system must be

$$\bar{P}_m = N + {}^{E}/_{N} + {}^{1}/_{T} \quad \text{(terms in dB)} \qquad (27)$$

$$\bar{P}_m \text{ [dB]} = 47.4 - 203 = -155.6 \text{ dBw}$$

This is the value which will be used in the transmitter power calculation. It is assumed that individual receiver bandwidths need only be of the order $B \sim n_p \frac{1}{T} \sim 3000\text{Hz}$.

We have in a sense used only frequency diversity. One disadvantage of this system is the following. Assume the propagation channel bandwidth is 1 MHz. Then the total RF bandwidth must be greater than 2 MHz (for 3 frequencies). This could be in conflict with frequency allocation space in the GHz range. One could easily envision an equivalent time diversity system with the same signal to noise ratio but a data rate reduced by a factor of 3. (the total RF bandwidth here would be only of the order of 10 KHz). To keep the logistics simple, spaced antenna, angle of arrival, polarization and multipath diversity have not been considered. A combination of these methods could of course provide economy of transmitter power at the expense of complicating the operational details

I. Sample Transmitter Sizing Calculations

We will assume that the scattering angle is 6.2° and the antenna beamwidth $\sim 1.5^{\circ}$. Then

		f = 3 GHz	f = 4 GHz	f = 5 GHz	
Minimum Received Signal					
	$N = kT_{op}$	-203 dBw	-203	-203	-203
	E_b / NT	+47.4 dB	+47.4	+47.4	+47.4
Antenna Parameters					
Gain	$G_R G_T$	-84.6 ($d \sim 4^+$ meters)	-84.6 ($d \sim 3^+$ meters)	-85.7 ($d \sim 2.6$ meters)	-92.6 ($d \sim 4.0$ meters)
Antenna Efficiency	$L_T L_R$	+ 6.0	+ 6.0	+ 6.0	+ 6.0
Antenna-to-Medium Coupling		+ 9.0	+ 9.0	+ 9.0	+14.0
Free Space Power Loss					
	L_{pf}	+158.2	160.7	162.6	162.6
Propagation Channel Loss					
Gaseous and Rain Attenuation	$L_{G,R}$	+3.2	+4.2	+5.7	+5.7
Cross Section σ		-13.6	-14.0	-14.35	-14.25
Distance Dependence - $\frac{d^2}{4\pi \lvert \vec{X}' \rvert^2 \lvert \vec{d}-\vec{X}' \rvert^2}$		+115.2	+115.2	+115.2	+115.2
Required Transmitter Powers		+37.8 dBw or 6 KW	+40.9 12.3 KW	+42.85 19.3 KW	+41.0 12.0 KW

It is seen (with the exception of the 2.6m antenna at 5 GHz) all the computations give values in the neighborhood of 10 KW. We feel that these values are rather conservative values for the following reasons.

(a) The cross section σ was derived on the basis that only the tropopause layer contributed to the scattering. Obviously both the 'weaker' stratospheric

and upper troposphere layers will contribute significantly.

(b) There may be no need for such a high data rate (1000 bits/sec. normal). Hence we could either reduce the bit rate (to as low 100 bits/sec. and 10 bits/sec) and pick up as much as 20 dB or we could increase the probability of error from 10^{-3} to 10^{-2} and save 4.7 dB (or we could do both). Certainly we could adopt other diversity schemes provided that they are consistent with the operational requirements desired.

III. RECOMMENDATIONS

We have shown that a mobile troposcatter system with a moderately long link range (640 km) and an information bit rate of the order of 1000 bits/sec is feasible. This is a rather uncommon type of troposcatter system.

We advocate further research being done in tropospheric scattering from the tropopause and stratospheric regions (particularly in the 2 to 8 GHz region). It is felt that the results from scatter experiments in this area will provide the fundamental basis for a class of operationally flexible troposcatter systems.

APPENDIX A

Essential Equations of Scattering Theory

The following few paragraphs outline the derivation of the equation for the power scattered by the refractive index inhomogeneities in the common volume $V_{R'}$ formed by the intersection of two narrow antenna beams. If $\frac{\partial \epsilon}{\partial t} \ll \omega \epsilon$ the wave equation can be written as

$$\nabla \times \nabla \times \underset{\rightarrow}{E}(\underset{\rightarrow}{r}) - k_o^2 \underset{\rightarrow}{E}(\underset{\rightarrow}{r}) = k_o^2 \left(\frac{\epsilon(\underset{\rightarrow}{r})}{\epsilon_o} - 1\right) \underset{\rightarrow}{E}(\underset{\rightarrow}{r}) = \frac{k_o^2}{\epsilon_o} \underset{\rightarrow}{P}(\underset{\rightarrow}{r}) \qquad (a\text{-}1)$$

A small perturbation technique (the Born approximation) is used to solve this equation. The electric field is broken into separate incident and scattered components and the 1st order equation becomes

$$\nabla \times \nabla \times \underset{\rightarrow}{E}^{sc}(\underset{\rightarrow}{r}) - k_o^2 \underset{\rightarrow}{E}^{sc}(\underset{\rightarrow}{r}) = \begin{cases} 0 \text{ if } (r \notin V_{R'}) \\ \\ \dfrac{k_o^2}{\epsilon_o} \underset{\rightarrow}{P}^{incid.}(r, r') \text{ if } (r \in V_{r'}) \end{cases} \qquad (a\text{-}2)$$

The standard method of solving the above equation is to use the well known Green's identity, which in turn first requires finding the simpler Green's dyadic solution[†]. Now to solve the equations for the Green's dyadic, one uses Fourier transform calculus along with the usual complex function theoretic arguments. If only the far field terms are included the scattered field turns out to be

---

[†] The equations for the Green's dyadic (and its compatibility equation) are given in Cartisian tensor notation.

$$\left\{ \frac{\partial^2}{\partial X_i \partial X_j} - \frac{\partial}{\partial X_p \partial X_p} - k_o^2 \right\} \Gamma_{im} = \delta_{im} u_o(r_g', r_g, t, t')$$

$$k_o^2 \frac{\partial}{\partial X_i} \Gamma_{im} = - \delta_{im} \frac{\partial}{\partial X_i} u_o(r_g, r_g', t, t')$$

$$E_i^{sc}(r_g, t) = \frac{k_o^2 e^{-j\omega t}}{4\pi} \int_{V_{R'}} \left\{ \frac{\delta_{im}}{|\underset{\rightarrow}{r} - \underset{\rightarrow}{r}'|} - \frac{(r_i - r_i')(r_m - r_m')}{|\underset{\rightarrow}{r} - \underset{\rightarrow}{r}'|^3} \right\}$$

$$\times \left\{ \frac{\epsilon(r_g')}{\epsilon_o} - 1 \right\} E_m^{inc}(r_g') e^{jk_o|\underset{\rightarrow}{r} - \underset{\rightarrow}{r}'|} dV_{R'} \qquad \text{(a-3)}$$

where

$$|\underset{\rightarrow}{r} - \underset{\rightarrow}{r}'| \triangleq \sqrt{(r_j - r_j')(r_j - r_j')} .$$

In equation a-3, $\underset{\rightarrow}{r}$ refers to the field point where E^{sc} is measured and $\underset{\rightarrow}{r}'$ refers to the scattering source point. It is clear that E_m^{inc} is an inconvenient variable and should be related to the field near the transmitter or better yet to the total power radiated. The geometry to be used and the symbols are shown in Fig. 18. The transmitter (A) is the origin of the coordinate system. Using the notation of Fig. 18, the electric field at the receiver can be expressed as

$$\underset{\rightarrow}{E}(\underset{\rightarrow}{d}, t) = \frac{k_o^2 e^{-j\omega t}}{4\pi} \int_{V_{R'}} \frac{\delta\epsilon(\underset{\rightarrow}{x}')}{\epsilon_o} \frac{\underset{\rightarrow}{a}_D(\underset{\rightarrow}{k}_r)\sin\chi\,|E(0)|}{|\underset{\rightarrow}{r}|\,|\underset{\rightarrow}{x}'|}$$

$$\times e^{j\{(\underset{\rightarrow}{k}_x - \underset{\rightarrow}{k}_r)\cdot\underset{\rightarrow}{x}' + \underset{\rightarrow}{k}_r\cdot\underset{\rightarrow}{d}\}} dV_R \qquad \text{(a-4)}$$

where $V_{R'}$ is the common volume and $|E(0)|$ is the magnitude of the field at the transmitter. Since the beams are narrow ($\sim 1^o$) one can make the approximations

$$\text{a)} \quad \underset{\rightarrow}{k}_{x'} = \underset{\rightarrow}{k}_{X'} \text{ and } \underset{\rightarrow}{k}_r = \underset{\rightarrow}{k}_R \quad \text{for all } x' \in V_{R'}$$

$$\text{b)} \quad G_r(k_{x'}) = G_T(k_{X'}),\ G_R(k_r) = G_R(k_R) \qquad \text{(a-5)}$$

The field at the receiver feed $\underset{\rightarrow}{E}_R(d,t)$ is then related to the field at the transmitter feed $\underset{\rightarrow}{E}_T(0)$ by

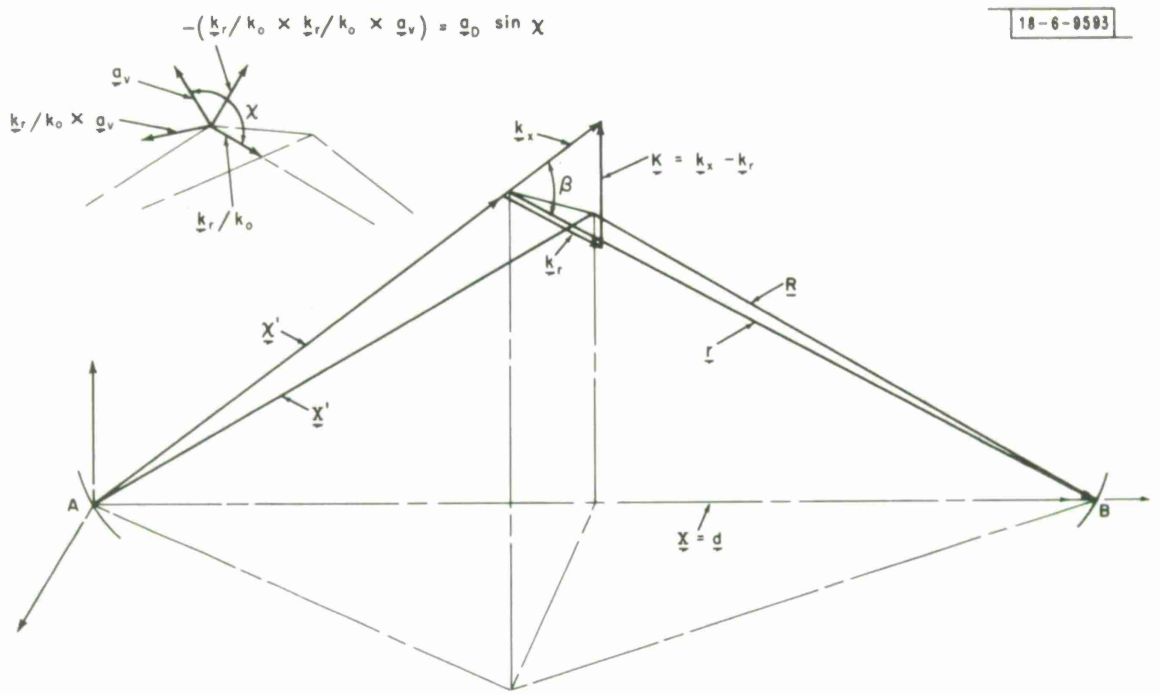

Fig. 18. Beam geometry.

$$\underset{\rightarrow}{E}_R(\underset{\rightarrow}{d},t) = \frac{\underset{\rightarrow}{a}_D \sin\chi\,|E_T(0)|\,k_o^2\sqrt{G_T G_R}\;\lambda}{(4\pi)\;|\underset{\rightarrow}{X}'|\;|\underset{\rightarrow}{d}-\underset{\rightarrow}{X}'|\sqrt{4\pi}}\; e^{-j(\omega t - \underset{\rightarrow}{k}_R\cdot\underset{\rightarrow}{d})} \int_{x'}$$

$$\times\;\frac{\delta\epsilon(\underset{\rightarrow}{x}')}{\epsilon_o}\, e^{j(\underset{\rightarrow}{k}_{X'}-\underset{\rightarrow}{k}_R)\cdot\underset{\rightarrow}{x}'}\, d\underset{\rightarrow}{x}' \qquad (a\text{-}6)$$

The usual practice is then to form $\underset{\rightarrow}{E}_R\cdot\underset{\rightarrow}{E}_R^{*}$ and normalize by $(\underset{\rightarrow}{E}\cdot\underset{\rightarrow}{E}^{*})_{fs}$ which is proportional to the power that would be received on a line-of-sight transmission between the antennas. The free space power is proportional to

$$(\underset{\rightarrow}{E}\cdot\underset{\rightarrow}{E}^{*})_{fs} \equiv |E_T(0)|^2 G_T G_R \left(\frac{\lambda}{4\pi d}\right)^2 \qquad (a\text{-}7)$$

Now $\frac{\delta\epsilon}{\epsilon_o} = 2N\times 10^{-6}$ and hence the final power equation reduces to

$$\frac{P(\underset{\rightarrow}{d})}{P_{fs}} = \frac{\underset{\rightarrow}{E}_R\cdot\underset{\rightarrow}{E}_R^{*}}{(E\cdot E^{*})_{fs}} = \frac{\sin^2\chi\, K^4 d^2\, 10^{-12}}{16\pi\sin^4\frac{\beta}{2}\,|\underset{\rightarrow}{X}'|^2\,|\underset{\rightarrow}{d}-\underset{\rightarrow}{X}'|^2}\int_V\int_{V'} N(\underset{\rightarrow}{x}')\times$$

$$N(\underset{\rightarrow}{x}'')\, e^{+j\underset{\rightarrow}{K}\cdot(\underset{\rightarrow}{x}'-\underset{\rightarrow}{x}'')}\, d\underset{\rightarrow}{x}''d\underset{\rightarrow}{x}' \qquad (a\text{-}8)$$

where $\underset{\rightarrow}{K} = \underset{\rightarrow}{k}_x - \underset{\rightarrow}{k}_R$ and $K = 2k_o\sin\frac{\beta}{2}$.

It must be recognized that equation (a-8) is appropriate for a particular spatial distribution of the refractive index and accordingly both $N(\underset{\rightarrow}{x};t)$ and $P(\underset{\rightarrow}{d})$ are random variables. As yet the structure of turbulence in the common volume ($V_{R'}$) has not been specified. Let us consider the term

$$\int_{V'}\int_{V''} N(\underset{\rightarrow}{x}')\,N(\underset{\rightarrow}{x}'')\, e^{-j\underset{\rightarrow}{K}\cdot(\underset{\rightarrow}{x}'-\underset{\rightarrow}{x}'')}\, d\underset{\rightarrow}{x}''\, d\underset{\rightarrow}{x}' .$$

If $N(\underset{\rightarrow}{x}')$ is a constant this expression is zero for $K \neq 0$ (which one expects physically). A cumulative distribution function $F_N(\underset{\rightarrow}{x}', \underset{\rightarrow}{x}'')$ is assumed and one then determines the expectation

$$\int\int E[N(\underset{\rightarrow}{x}')N(\underset{\rightarrow}{x}")]\, e^{-j\underset{\rightarrow}{K}\cdot(x'-x")}\, d\underset{\rightarrow}{x}"\, d\underset{\rightarrow}{x}' = \int\int e^{+j\underset{\rightarrow}{K}\cdot(\underset{\rightarrow}{x}'-\underset{\rightarrow}{x}")}$$

$$\times \left\{ \text{cov}\, N(\underset{\rightarrow}{x}')\, N(\underset{\rightarrow}{x}") + E\,N(\underset{\rightarrow}{x}')\, E\,N(\underset{\rightarrow}{x}") \right\} d\underset{\rightarrow}{x}"\, d\underset{\rightarrow}{x}' \qquad \text{(a-9)}$$

The second term on the right side of equation (a-9) becomes zero under the integration process. If the field is locally spatially homogeneous (in the wide sense) one can write $\text{cov}[N(\underset{\rightarrow}{x}')N(\underset{\rightarrow}{x}")] = R_N(\underset{\rightarrow}{x}', \underset{\rightarrow}{x}")$ where $R_N(\cdot\,,\cdot)$ is the correlation coefficient.

$$\text{cov}\,[N(\underset{\rightarrow}{x}')\,N(x")] = R_N(\underset{\rightarrow}{x}' - \underset{\rightarrow}{x}",\, 0) = R_N(\underset{\rightarrow}{x}' - \underset{\rightarrow}{x}") \qquad \text{(a-10)}$$

Now we perform a change of variables $(\underset{\rightarrow}{x}', \underset{\rightarrow}{x}") \rightarrow (\underset{\rightarrow}{\xi}, \underset{\rightarrow}{\gamma})$ where $\underset{\rightarrow}{\xi} = \underset{\rightarrow}{x}' - \underset{\rightarrow}{x}"$ and $\underset{\rightarrow}{\gamma} = \dfrac{\underset{\rightarrow}{x}' + \underset{\rightarrow}{x}"}{2}$. The Jacobian for the change of coordinates turns out to be equal to 1 hence;

$$\int_{V_{x"}}\int_{V_{x'}} E[N(\underset{\rightarrow}{x}')\,N(\underset{\rightarrow}{x}")]\, e^{+j\underset{\rightarrow}{K}\cdot(\underset{\rightarrow}{x}'-\underset{\rightarrow}{x}")}\, d\underset{\rightarrow}{x}'\, d\underset{\rightarrow}{x}" \cong \int_{V_{x"}} \left[\int_{V_{\xi}}\right.$$

$$\left. \times\, R_N(\underset{\rightarrow}{\xi})\, e^{+j\underset{\rightarrow}{K}\cdot\underset{\rightarrow}{\xi}}\, d\underset{\rightarrow}{\xi} \right]\, d\underset{\rightarrow}{\gamma}\,.$$

The normalized autocorrelation coefficient $\rho_N(.)$ is defined by

$$R_N(\underset{\rightarrow}{\xi}) \equiv E[N^2]\ \rho_N(\underset{\rightarrow}{\xi}) \equiv \overline{(N^2)}\ \rho_N(\underset{\rightarrow}{\xi})$$

where $\overline{(N^2)}$ can have slowly varying spatial dependence. A spectrum $\Phi_N(K)$ of the autocorrelation function is defined by

$$\frac{1}{8\pi^3}\int \rho_N(\underset{\rightarrow}{\xi})\, e^{j\underset{\rightarrow}{K}\cdot\underset{\rightarrow}{\xi}}\, d\underset{\rightarrow}{\xi} = \Phi_N(\underset{\rightarrow}{K}) \qquad \text{(a-11)}$$

where it is assumed that ρ_N decreases rapidly with $|\xi|$. Therefore

$$\int\int E[N(\underset{\rightarrow}{x}')N(\underset{\rightarrow}{x}'')]\, e^{-j\underset{\rightarrow}{K}\cdot(\underset{\rightarrow}{x}'-\underset{\rightarrow}{x}'')}\, d\underset{\rightarrow}{x}''\, d\underset{\rightarrow}{x}' = (2\pi)^3 \Phi(\underset{\rightarrow}{K}) \int_{V_\gamma}$$

$$\times\ \overline{(N^2)}\, d\underset{\rightarrow}{\gamma}\ . \qquad \text{(a-12)}$$

Therefore equation a-8 can be written as

$$\frac{P(\underset{\rightarrow}{d})}{P_{fs}} \cong 8\pi^2 \left(\frac{10^{-12} d^2}{|\underset{\rightarrow}{X}'|^2\, |\underset{\rightarrow}{d}-\underset{\rightarrow}{X}'|^2}\right) \left(\frac{K^4 \sin^2\chi}{(2\sin\frac{\beta}{2})^4}\right) \Phi_N(\underset{\rightarrow}{K}) \int_{V_\gamma} \overline{(N^2)}\, d\gamma \qquad \text{(a-13)}$$

If the turbulence has the same intensity throughout the common volume then

$$\frac{P(\underset{\rightarrow}{d})}{P_{fs}} \cong 8\pi^2 \left\{\frac{10^{-12} d^2}{|X'|^2\, |d-X'|^2}\right\} \left\{\frac{K^4 \sin^2 X}{(2\sin\frac{\beta}{2})^4}\right\} \Phi_N(\underset{\rightarrow}{K}) \overline{(N^2)}\ V \qquad \text{(a-14)}$$

The equation for bistatic scattering if path and system losses are ignored is

$$P(\underset{\rightarrow}{d}) = \frac{P_t G_t G_r \lambda^2 \sigma}{(4\pi)^3 |\underset{\rightarrow}{X}'|^2\, |\underset{\rightarrow}{d}-\underset{\rightarrow}{X}'|^2} \qquad \text{(a-15)}$$

Normalized by the free space power we get

$$\frac{P(d)}{P_{fs}} = \frac{\sigma d^2}{|\underset{\rightarrow}{X}'|^2\, |\underset{\rightarrow}{d}-\underset{\rightarrow}{X}'|^2 (4\pi)} \qquad \text{(a-16)}$$

If equation a-16 and a-14 are combined, the bistatic cross section turns out to be

$$\sigma = 4(2\pi)^3 (10^{-12}) \left\{\frac{K}{(2\sin\frac{\beta}{2})}\right\}^4 \sin^2\chi\ \overline{(N^2)}\, V \Phi_N(\underset{\rightarrow}{K}) \qquad \text{(a-17)}$$

Since $k_o = \frac{2\pi}{\lambda} = \frac{K}{2\sin\frac{\beta}{2}}$ the above equation can be written as

$$\sigma = (4(2\pi)^7 . 10^{-12}) \frac{\sin^2\chi}{\lambda^4}\ \overline{(N^2)}\ V \Phi_N(\underset{\rightarrow}{K})$$

or

$$\sigma \triangleq \{(2.10^{-6})^2 \overline{(N^2)}\}\, 8\pi^3 k^4 \sin^2 \chi\, V \Phi_N(\vec{K})$$

This result came from assuming that the turbulence was uniform over the volume V and is the most common formula for the scattering cross section. We will use a slightly different version which is consistent with that of Tartarski. Instead of N units we will use the refractive index η and re-write equation a-8 as

$$\frac{\overline{P(\vec{d})}}{P_{fs}} = \frac{\sin^2 \chi\, K^4 d^2}{(4)(16\pi) \sin^4 \frac{\beta}{2} |\vec{X}'|^2 |\vec{d} - \vec{X}'|^2} \int_{V_{x'}} \int_{V_{x''}}$$

$$\times E[\eta(\vec{x}')\eta(\vec{x}'')]\, e^{+j\vec{K}\cdot(\vec{x}' - \vec{x}'')}\, d\vec{x}''\, d\vec{x}' \qquad (a\text{-}18)$$

and let

$$\int_{V_{x'}} \int_{V_{x''}} E[\eta(\vec{x}')\eta(\vec{x}'')]\, e^{j\vec{K}\cdot(\vec{x}' - \vec{x}'')}\, d\vec{x}''\, d\vec{x}' = \int_{V_\gamma} \overline{\eta^2(\chi)} \int_{V_\xi}$$

$$\times \rho_N(\vec{\xi})\, e^{j\vec{K}\cdot(\vec{\xi})}\, d\vec{\xi}\, d\chi \triangleq 8\pi^3 \int_{V_\gamma} \Phi_\eta(\vec{K}, \vec{\gamma})\, d\vec{\gamma}. \qquad (a\text{-}19)$$

Then

$$\frac{\overline{P(\vec{d})}}{P_{fs}} = \frac{\pi^2 \sin^2 \chi\, K^4 d^2}{8 \sin^4 \frac{\beta}{2} |\vec{X}'|^2 |\vec{d} - \vec{X}'|^2} \int_{V_\gamma} \Phi_\eta(\vec{K}, \chi)\, d\chi \qquad (a\text{-}20)$$

and

$$\sigma = \frac{\pi^3}{2} \frac{\sin^2 \chi}{\sin^4 \frac{\beta}{2}} K^4 \int_{V_\gamma} \Phi_\eta(\vec{K}, \chi)\, d\chi = 8\pi^2 \sin^2 \chi\, k^4 \int_{V_\gamma}$$

$$\times \Phi_\eta(\vec{K}, \chi)\, d\chi \ . \qquad (a\text{-}21)$$

In terms of dB the appropriate expression to be used is then

$$\overline{P(d)} = P_{fs}[\mathrm{dB}] + 10\log_{10}\frac{d^2}{4\pi\,|\underset{\rightarrow}{d} - \underset{\rightarrow}{X'}|^2\,|\underset{\rightarrow}{X'}|^2} + \sigma\,[\mathrm{dB}]\,. \qquad \text{(a-22)}$$

APPENDIX B

Approximate Geometry of the Common Volume

A few useful but approximate formulas for the common volume (for narrow beam antennas) are given below. The beams are assumed to be rectangular in the plane transverse to the beam axis. The area of face ABCD is given by

$$A(ABCD) \simeq \frac{(d_r \hat{\theta}_{V,r})(d_t \hat{\theta}_{V,t})}{\sin \beta} .$$

The width of the common volume is determined primarily by the narrowest beam. Define

$$W \cong d\hat{\theta}_H = \min (d_r \hat{\theta}_{H,r}, d_t \hat{\theta}_{H,t}).$$

The volume of the common volume is approximately

$$V \simeq d\hat{\theta}_H \frac{(d_r \hat{\theta}_{V,r})(d_t \hat{\theta}_{V,t})}{\sin \beta} \qquad \text{(b-1)}$$

If the geometry shows perfect symmetry $d = D/2$; $\theta = \theta_{V,R} = \theta_{H,R} = \theta_{V,T} = \theta_{V,R}$

$$V \simeq \frac{D^3 \hat{\theta}^3}{8 \sin \beta} \qquad \text{(b-2)}$$

Another useful formula is the area of a horizontal layer which is limited by the common volume geometry.

$$A_L \simeq \frac{2(\Delta Z)}{\tan \frac{\beta}{2}} \cdot \frac{D}{2} \hat{\theta}_H = \frac{(\Delta Z) D \hat{\theta}_H}{(\tan \frac{\beta}{2})} . \qquad \text{(b-3)}$$

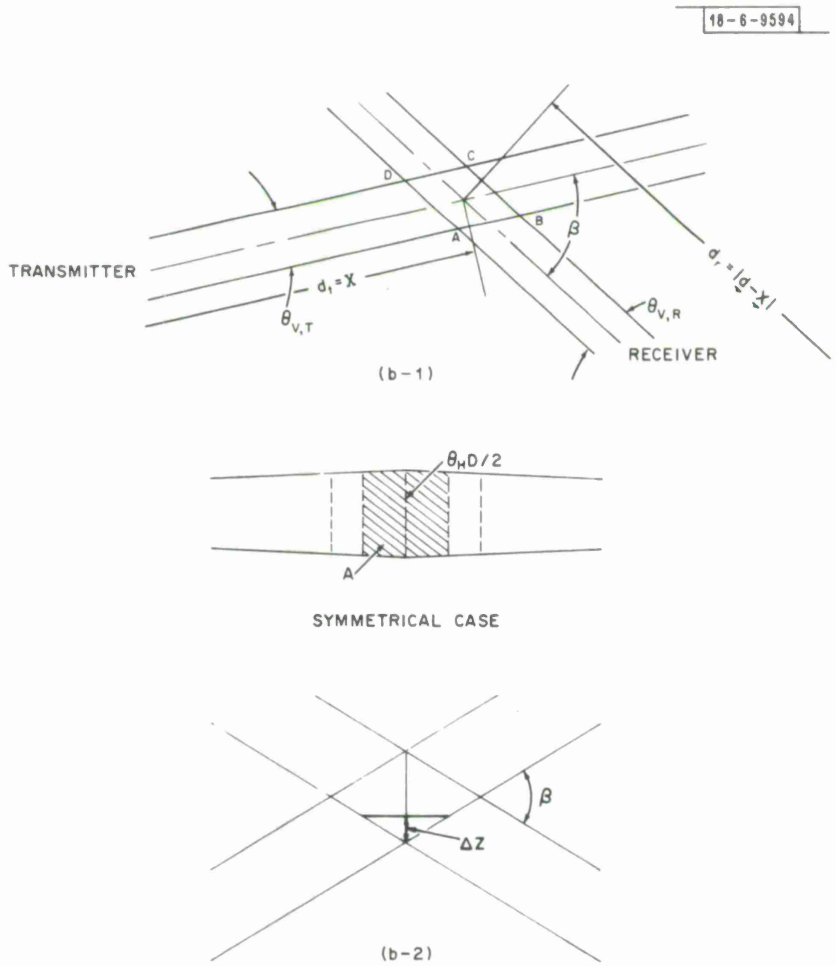

Fig. 19. Common volume geometry.

For any two ray paths, the maximum path difference is given by

$$\Delta l \simeq \left(\frac{d_t \hat{\theta}_{V,t}}{\sin \beta} - \frac{d_r \hat{\theta}_{V,r}}{\tan \beta}\right) + \left(\frac{d_r \hat{\theta}_{V,r}}{\sin \beta} - \frac{d_t \hat{\theta}_{V,t}}{\tan \beta}\right).$$

For the case of beam geometry symmetry

$$\Delta l \simeq D \hat{\theta} \tan \frac{\beta}{2} . \qquad \text{(b-4)}$$

REFERENCES

1. B. Bean and E. Dutton, Radio Meteorology, National Bureau of Standards Monograph 92 U. S. Government Printing Office.

2. W. Gordon, "Physical Characteristics of the Troposphere," Radio Wave Propagation in the Troposphere, J. Saxon, ed. (Elsevier Publishing Co., New York, 1962).

3. L. P. Yeh, "Experimental Aperature-to-Medium Coupling Loss," IEEE Transactions on Antennas and Propagation, 663 (September 1966).

4. F. DuCastel, Tropospheric Radiowave Propagation beyond the Horizon, Pergamon Press, New York (1966).

5. H. Booker and W. Gordon, "A Theory of Radio Scattering in the Troposphere," Proc. IRE, 401-412 (April 1950).

6. R. Bolgiano, "Wavelength Dependence in Transhorizon Propagation," Proc. IRE, 47, 331-332 (1959).

7. V. Tartarski, Wave Propagation in a Turbulent Medium, McGraw Hill, New York (1961).

8. G. Bachelor, The Theory of Homogeneous Turbulence, Cambridge University Press (1959).

9. R. Crane, "Monostatic and Bistatic Scattering from Thin Turbulent Layers in the Atmosphere," M. I. T. Lincoln Laboratory Technical Note TN 1968-34 (September 1968).

10. K. Norton, P. Rice and L. Vogler, "The Use of Angular Distance in Estimating Transmission Loss and Fading Range for Propagation Through a Turbulent Atmosphere...," Proc. IRE, 43, 1488-1526 (October 1955).

11. J. Greene and M. Lebenbaum, Letter to the Editor, Microwave Journal, 2, 13 (October 1959).

12. J. N. Pierce, "Theoretical Diversity Improvement in Frequency-Shift Keying," Proc. IRE, 46, 933 (1958).

DOCUMENT CONTROL DATA – R&D

(Security classification of title, body of abstract and indexing annotation must be entered when the overall report is classified)

1. ORIGINATING ACTIVITY *(Corporate author)* Lincoln Laboratory, M.I.T.	2a. REPORT SECURITY CLASSIFICATION Unclassified 2b. GROUP None

3. REPORT TITLE

Feasibility of Low Data Rate Mobile Troposcatter Communication Systems

4. DESCRIPTIVE NOTES *(Type of report and inclusive dates)*
Technical Note

5. AUTHOR(S) *(Last name, first name, initial)*

White, David P.

6. REPORT DATE 30 April 1969	7a. TOTAL NO. OF PAGES 62	7b. NO. OF REFS 12
8a. CONTRACT OR GRANT NO. AF 19(628)-5167 b. PROJECT NO. 1508A c. d.	9a. ORIGINATOR'S REPORT NUMBER(S) Technical Note 1969-15 9b. OTHER REPORT NO(S) *(Any other numbers that may be assigned this report)* ESD-TR-69-77	

10. AVAILABILITY/LIMITATION NOTICES

This document has been approved for public release and sale; its distribution is unlimited.

11. SUPPLEMENTARY NOTES None	12. SPONSORING MILITARY ACTIVITY U.S. Navy

13. ABSTRACT

For a communications system with a low data rate requirement (i.e., 1 – 1000 bits/sec) one can use troposcatter links over a range interval beyond the distances commonly used. The range is limited by the requirement that the tropopause layer is to be included in the common volume of the beams. This effectively limits the range in most cases to about 450 miles. It is proposed to use frequencies in the interval 3 to 5 GHz. This enables one to specify a completely mobile troposcatter system since the antenna paraboloids have diameters of the order of 10 feet and the power requirement is a modest 10 kW.

14. KEY WORDS

communication systems

tropospheric scatter